

Renewable Energy and Engines Lab
Department of Mechanical Engineering
Statesboro, Georgia, USA



Allen E. Paulson College of Engineering

Analysis of Horizontal Axis Wind Turbine Array Optimization

Peter-Claver Nwanze, Ed.D.

Keith Bazemore, M.S.

Jessica Lyons, M.Ed.

J. Ann Mitchem, B.S.Ed, M.Ed (Candidate)

Drake Grall, Matthew Kiernan, Yakub Sharif (Mentors)

Summer 2019

Valentin Soloiu, Ph.D (P.I.)

Mosfequr Rahman, Ph.D (Supervisor)



NSF-RET #1609524

Engaging Educators in Renewable Energy

Table of Contents

Abstract	2
Introduction	3
Experimental Methods	4
Results	6
Discussion	7
Conclusion	8
Appendices	
Appendix A - Flow Chart	9
Appendix B - Array Schematics	10
Appendix C - Tables of Average Output	12
Appendix D - Charts of Average Output	14
Appendix E - Power Coefficient Charts	18
Appendix F - Data Graphs by Trial	19

ABSTRACT

Wind energy is the fastest growing form of renewable energy, with a multitude of possibilities for expansion. This, as well as other forms of renewable energy, will facilitate understanding of the growing concerns regarding global warming by decreasing our dependence on fossil fuels. Wind energy requires wind speeds of at least six miles per hour; therefore, only certain geographical areas are suitable for the use of this technology. The purpose of this experiment was to determine whether the orientation of an array of wind turbines increases or decreases energy production and efficiency. In this study, various arrays consisting of five wind turbines were tested. The total energy output of each array was tested using a wind tunnel from the wind energy lab at Georgia Southern University, INA219 current sensors, custom software written by Matthew Kiernan, and five “Cutting Edge Power” wind turbines. The most efficient array in terms of voltage, power and current was the 2-1-2 array, with average outputs of: voltage at 3.98 V, current at 440.73 mA, and power at 900.92 mW. The efficiency was determined through the power coefficient, which was 32.64%. The next most efficient array was the Left-Right Staggered array, with averages of: voltage at 3.90 V, current at 208.47 mA, and power at 838.08 mW. The efficiency was determined through the power coefficient, which was 32.13%.

The Diagonal array was the third most efficient in overall energy output, with averages of: voltage at 3.75 V, current at 200.66 mA, and power at 789.07 mW. The efficiency was determined through the power

coefficient, which was 29.54. The least efficient array array for energy output was Single File, with averages of: voltage at 2.79 V, current at 137.69 mA, and power at 451.05 mW. The efficiency was determined through the power coefficient, which was 18.31%.

The results demonstrated that the close proximity of turbines negatively affects energy output, as observed through the turbulence that was produced. Possible errors observed were due to turbine models that did not perform as expected as well as the breadboard configuration.

INTRODUCTION

The primary types of renewable energy include biomass, geothermal, hydroelectricity, solar, and wind. Increasing the use of renewable energy will decrease our use of fossil fuels; thus decreasing carbon dioxide emissions and pollution [1]. As seen in Figure 1, as of 2017, 11% of the energy consumption in the United States came from renewable resources [2].

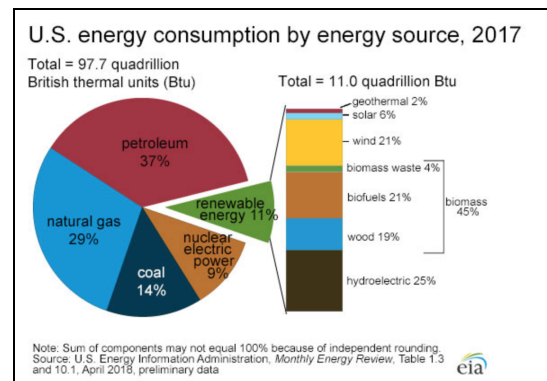


Figure 1. Graph of US energy consumption by source.

Present-day wind turbines are utilized to transform the kinetic energy of wind into electricity. Electricity generated from the wind is created by

converting kinetic energy from air flows that are found naturally within the Earth's atmosphere. This electricity is then produced by the wind turbine as the wind's kinetic energy rotates the turbine, which then converts it into mechanical energy. This rotation turns an internal shaft connected to a gear box. The gear box, in turn, spins a generator and produces electricity. The major components of a horizontal axis wind turbine (HAWT) can be seen in Figure 2.

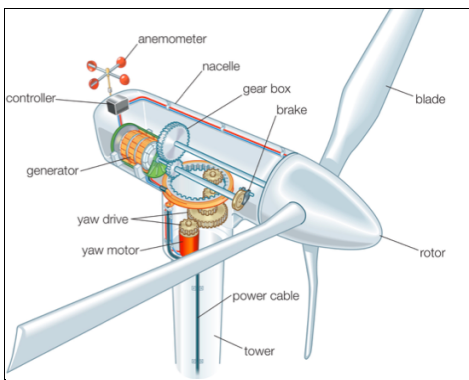


Figure 2. Dissected view of wind turbine components.

Wind turbines are typically around 262 feet tall. Steel towers support a nacelle, which houses the shaft, gear box, generator, and controls. Attached to the nacelle is a hub and at least two blades. To maximize energy production, the turbine is equipped with sensors that control rotation and maintain a perpendicular position to the strongest wind. The placement of the angle and pitch can also be adjusted to maximize the energy capture.

The wind speed required to generate electricity in a horizontal axis wind turbine is about six to nine miles per hour [1]. For this reason, the more popular locations for horizontal wind turbines include hilltops, open water, plains, and mountains.

In this investigation, attempts were made to determine the optimal configuration of a wind turbine array in relation to power, voltage, and current output, as well as efficiency. Wind turbine array performance is affected by two major factors: wake wind speed deficits and increased dynamic loads on the blades. This increased load is caused by higher turbulence. Downstream turbines are exceptionally affected by these factors. The inefficiency of the downstream turbines can be as much as 40% less than the turbines located most upstream. On average, power loss due to wake in wind arrays is between 10% and 20% [5].

The visible turbulence in Figure 3 below shows the dynamic turbulence that diminishes power output for downstream wind turbines. In Figure 4 below, a computer enhancement allows for a better understanding of the turbulence wake created by wind turbines.



Figure 3. Aerial view from the Southwest of wake clouds at Horns Rev, Denmark, February 12, 2008

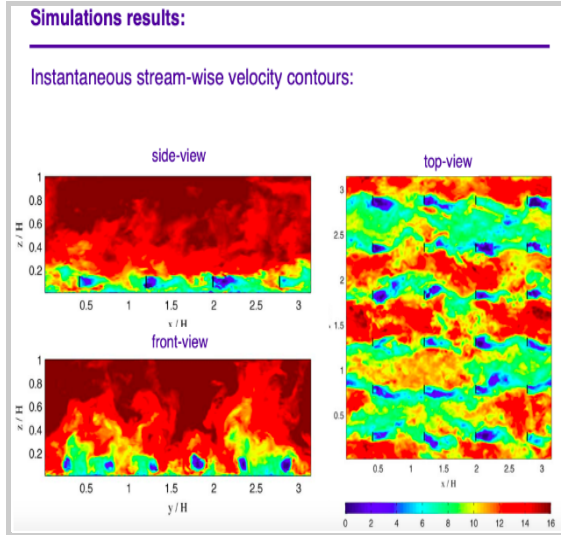


Figure 4. Computer enhancement of turbulence wake caused by wind turbines.

Early attempts to optimize array configurations simply used an intuitive rationale. Patel stated, from his research, that turbines should be spaced eight to twelve rotor diameters apart, viewing from the windward side, and one and one half to three rotor diameters apart, viewing from the crosswind side [7].

In contrast, Ammara's research suggests this to be an inefficient use of land. He proposed a denser, staggered siting scheme, which produces the same power on less land [8]. Most existing wind arrays are conveniently spaced six to ten rotor diameters apart in identical rows.

EXPERIMENTAL METHODS

In order to line the middle of the turbine up with the middle of the wind tunnel, the materials for the base were measured. Figure 5 below shows the sketch that was then drawn using the measurements. The height of the base included the height of the caster wheels attached to 5 cm x 10 cm blocks, the 3/4-in galvanized floor flange, the 93.3 cm galvanized support rod, and the

Cutting Edge turbine head. The center of the turbine was constructed to line up with the center of the wind tunnel at 104 cm from the floor.

In figures 6 and 7, the process can be seen as the group completed the measurements were made for four wind turbine array configurations, five turbines were used, the 122 cm x 244 cm piece of plywood was measured, and a 61 cm x 122 cm piece was cut to match wind tunnel width of 61 cm. The 3/4-in Galvanized Floor Flanges were set in the various array configurations with 1/4-in nuts, bolts, and washers.

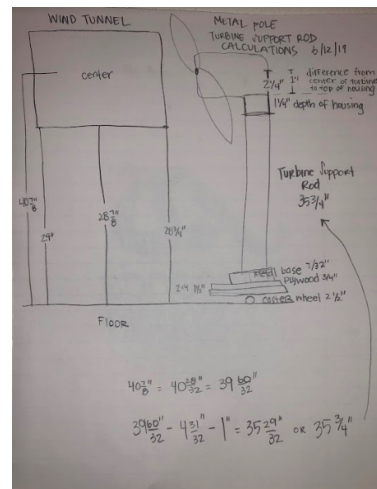


Figure 5. Design, sketch, and calculations for turbines.



Figure 6. Using table saw to cut out the base.



Figure 7. Measuring and designing array platform.

Various arrays were chosen to be tested during the experimental stage. The completed array platform can be seen in Figure 8 below.



Figure 8. Arrangement of mounted galvanized floor flanges for the various array configurations

For the first five turbine array configuration, the floor flange was set 6 cm from the front of our plywood platform. Lines were drawn 25.4 cm apart to indicate the separation distance from one turbine to the turbine behind it. This design represented the Single File configuration. The next array had the first turbine offset to the left 3 cm from the outer edge of the base, to keep the turbine blades from overlapping. The remaining four turbines would be placed with the same measurements, alternating from the right side to the left side of the plywood base - creating the Left-Right Staggered array. The third design was

called 2-1-2, where two turbines were placed next to each other in the front and rear rows and a single turbine was in the row between them. The final array design had the wind turbines placed diagonally from front left to back right, each with 25.4 cm between them, for the Diagonal design.

Once all of the trials were completed for each of the five turbine array configurations, the same four designs were arranged and tested with only three turbines. The first array was the Single File array, with each turbine placed in a line with one directly behind the other at 50.8 cm apart. The next array was arranged again with the first turbine offset to the left 3 cm from the outer edge of the base to keep the turbine blades from overlapping. The remaining two turbines would be placed with the same measurements, alternating from the right side to the left side of the plywood base - creating the Left-Right Staggered array. The third design was called 2-1, where two turbines were placed next to each other in the front row and a single turbine was in the center of the middle row. The final array design had the wind turbines placed diagonally from front left to back right, each with 25.4 cm between them, for the Diagonal design.

Once the arrays were constructed, with the flanges bolted in place, the first turbine support was cut at 90.8 cm from $\frac{3}{4}$ " galvanized steel pipe, using the horizontal band saw. One wind turbine assembly, with stand, was then put together and measured to ensure that the centers of the wind turbine and the wind tunnel exhaust were equal height.

Based on these measurements, it was determined that the height of the turbine assembly was off by 2.5 cm due to a calculation error. Thus, five support

rods were then cut to 93.3 cm instead of the original 90.8 cm.

Three trials, each three minutes in duration, were conducted for each of the four array configurations. Figure 9 shows the average wind speed of 10.64 meters per second (m/s). For the duration of each trial, the INA219 current sensors reported the voltage, current, and power output of each individual wind turbine at 100 millisecond intervals. This data was then sent via a USB cable to a computer that was operating on the custom software (designed by Matthew Kiernan and seen in Figures 11 and 12). The software system encompassed a virtual serial port that sorted each incoming data packet and then exported it into an Excel spreadsheet. Once the stop button in the software was pressed and the end-of-data packet was received, the spreadsheet was finalized and saved. The turbines were identified from front to rear as series 5 to series 1, respectively.



Figure 9. The wind tunnel at Georgia Southern University, with the anemometer reading 10.4 m/s.

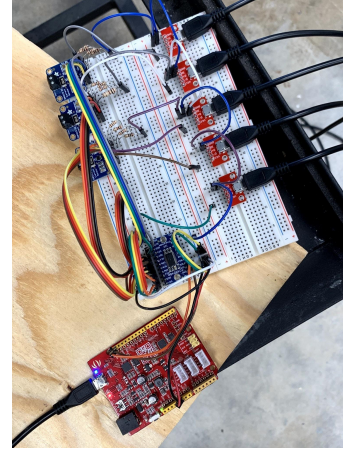


Figure 11. INA219 current sensors and custom software developed by Matthew Kiernan.

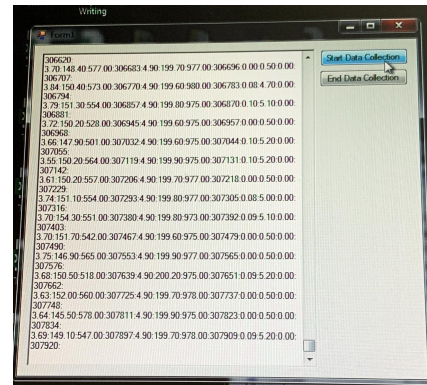


Figure 12. Software for data collection designed by Matthew Kiernan.

RESULTS

The most efficient array in terms of voltage, power and current was the 2-1-2 array, with average outputs of: voltage at 3.98 V, current at 440.73 mA, and power at 900.92 mW. The efficiency was determined through the power coefficient, which was 32.64%. The next most efficient array was the Left-Right Staggered array, with averages of: voltage at 3.90 V, current at 208.47 mA, and power at 838.08 mW. The efficiency was determined through the power coefficient, which was 32.13%.

The Diagonal array was the third most efficient in overall energy output, with averages of: voltage at 3.75 V,

current at 200.66 mA, and power at 789.07 mW. The efficiency was determined through the power coefficient, which was 29.54. The least efficient array for energy output was Single File, with averages of: voltage at 2.79 V, current at 137.69 mA, and power at 451.05 mW. The efficiency was determined through the power coefficient, which was 18.31%. Charts for these results can be seen in Figures 25-60 in Appendix F, Figures 17-19 in Appendix D, Tables 1-4 in Appendix C, and Figure 23 in Appendix F.

DISCUSSION

The most efficient array in terms of voltage, power and current was the 2-1-2 array, with average outputs of: voltage at 3.98 V, current at 440.73 mA, and power at 900.92 mW. The efficiency was determined through the power coefficient, which was 32.64%. The next most efficient array was the Left-Right Staggered array, with averages of: voltage at 3.90 V, current at 208.47 mA, and power at 838.08 mW. The efficiency was determined through the power coefficient, which was 32.13%.

The Diagonal array was the third most efficient in overall energy output, with averages of: voltage at 3.75 V, current at 200.66 mA, and power at 789.07 mW. The efficiency was determined through the power coefficient, which was 29.54. The least efficient array for energy output was Single File, with averages of: voltage at 2.79 V, current at 137.69 mA, and power at 451.05 mW. The efficiency was determined through the power coefficient, which was 18.31%. Charts for these results can be seen in Figures 25-60 in Appendix F, Figures 17-19 in

Appendix D, Tables 1-4 in Appendix C, and Figure 23 in Appendix F.

The “Cutting Edge Power” wind turbines were deemed adequate, but additional tests with other turbine models is recommended in order to determine which one would yield the most accurate results. The second turbine from the front, identified as series 4 in the array, seemed to produce ambiguous data. The ambiguity is most likely due to vibrations throughout the setup (i.e. turbine stand, blades, voltage regulator module, etc.).

In an attempt to reduce the variations in data, the same arrays were tested, but with only three wind turbines. Overall, the results were the same. The 2-1 array was still the most efficient with the highest averages for: voltage at 3.28 V, current at 133.47 mA, and power at 590.53 mW. The efficiency was determined through the power coefficient, which was 21.51%. The Left-Right Staggered was the next most efficient design, with averages of: voltage at 3.20 V, current at 130.53 mA, and power at 574.40 mW. The efficiency was determined through the power coefficient, which was 21.72%. The Diagonal array came in third, with averages of: voltage at 3.15 V, current at 127.78 mA, and power at 541.45 mW. The efficiency was determined through the power coefficient, which was 20.32%. The Single File array was the least efficient, with averages of: voltage at 2.75 V, current at 112.00 mA, and power at 455.15 mW. The efficiency was determined through the power coefficient, which was 18.31%.

In future experiments it would be ideal to use a higher quality wind turbine to reduce the noise or vibration. In addition, it is recommended to use a

printed circuit board (PCB) rather than a breadboard. Graphs 5, 6, and 7 indicate that the 2-1-2 array had the highest overall power output, highest overall voltage output, and the highest overall current output.

CONCLUSION

In this experiment, array efficiency was tested. Five “Cutting Edge Power” array wind turbines were arranged in various configurations; identified as Single file, 2-1-2, Left-Right Staggered, and Diagonal.

Using INA219 current sensors, custom software written by M. Kiernan and an average wind speed of 10.64 m/s, data were collected for power, current, and voltage for each of the five turbines respectively and collectively. Wind turbine efficiency is affected by the amount of turbulence generated by each turbine. Therefore, array design is critical for energy optimization.

The array designs that were most efficient in producing energy were the 2-1-2, and Left Right Staggered. This is due to more space between turbines creating less wake turbulence. The array that was least efficient was Single File.

APPENDIX A

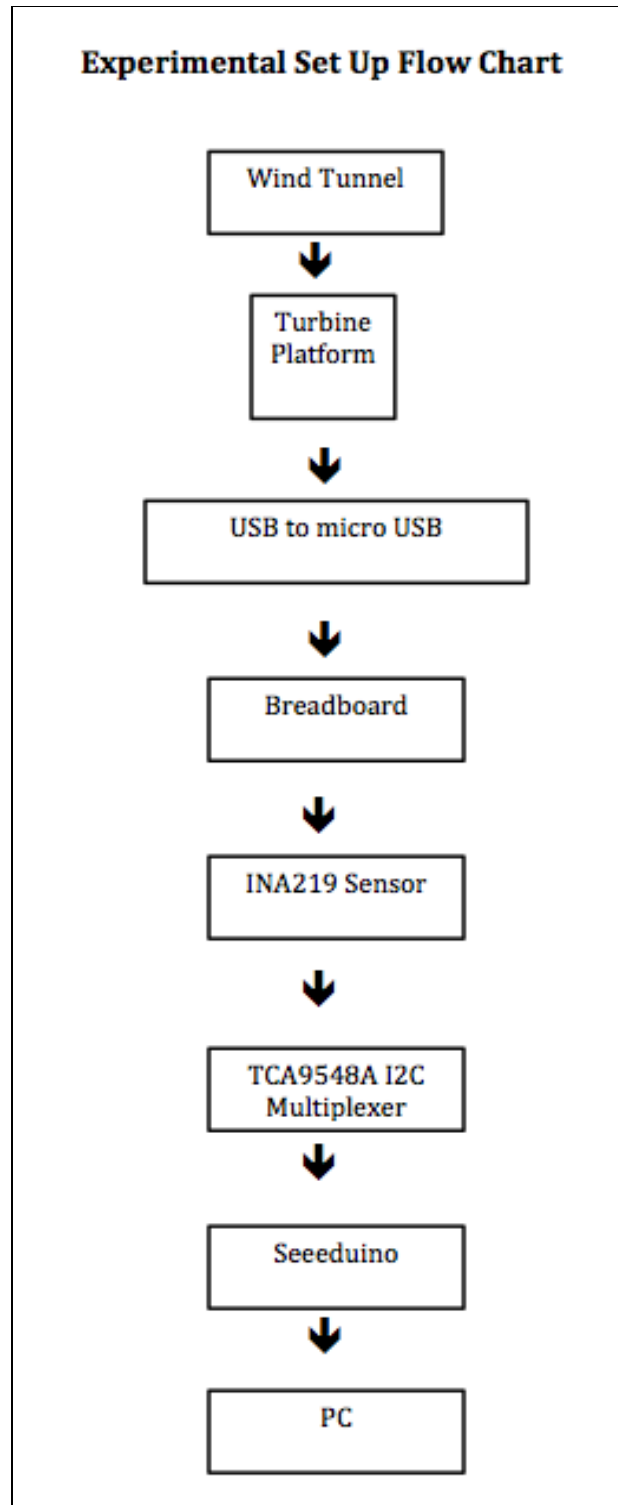


Figure 13. Experimental Design Flow Chart (used for 5 array and 3 array)

APPENDIX B

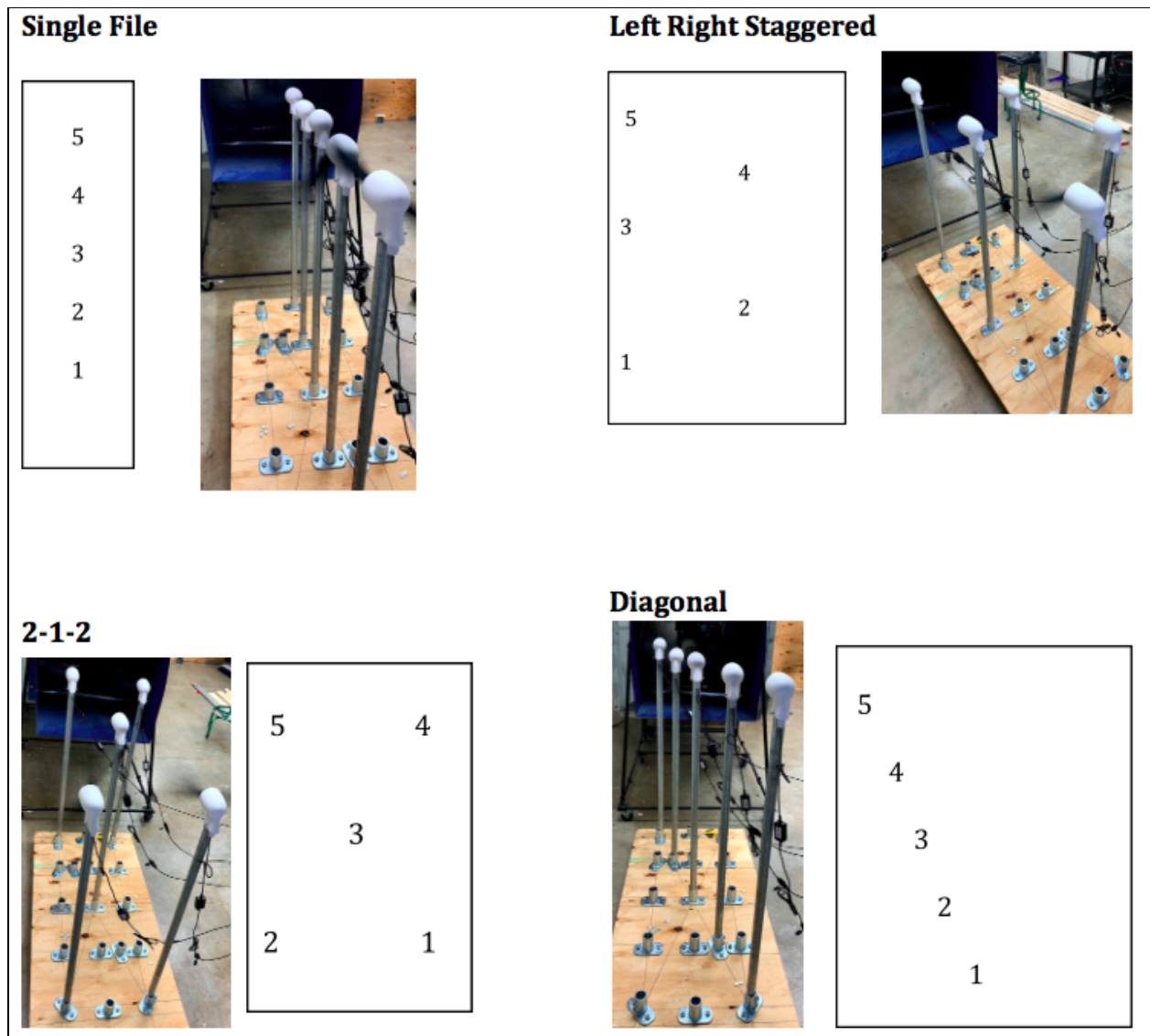
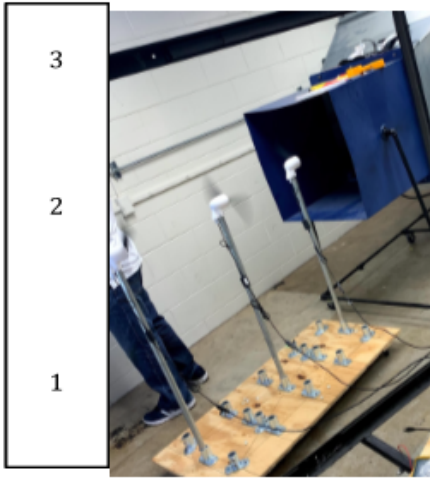
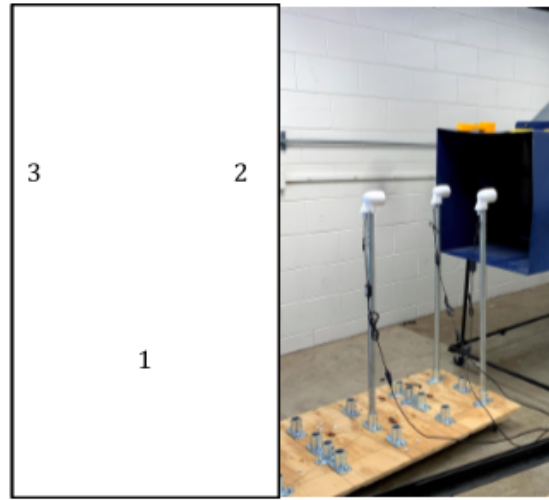


Figure 14. Five Turbine Array Schematics

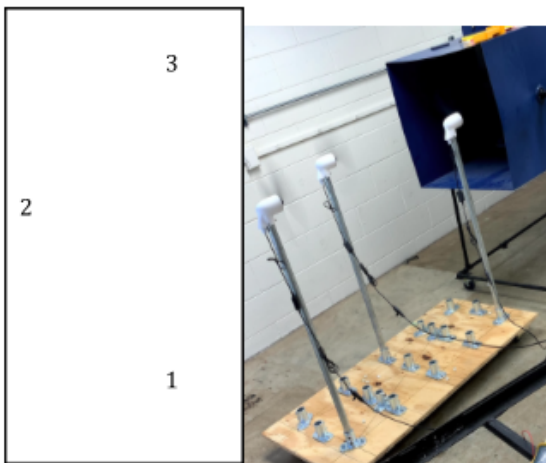
3 Array Single File



3 Array 2-1



3 Array Left Right Staggered



3 Array Diagonal

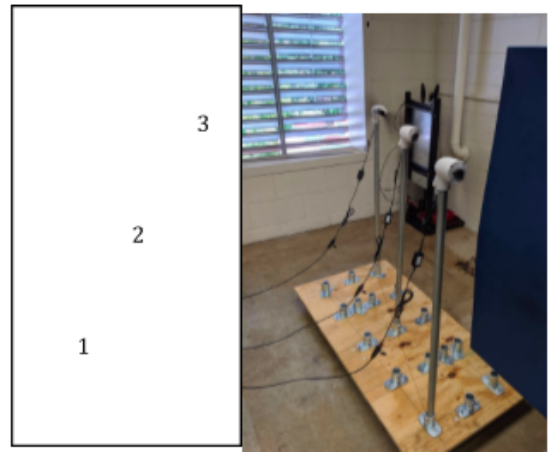


Figure 15. Three Turbine Array Schematics

APPENDIX C

Five Turbine Averages, by Array

Table 1. Results of Single File Array

	Single File			Average
	1	2	3	
Voltage (V)	2.76	2.82	2.78	2.79
Current (mA)	135.39	139.67	138.01	137.69
Power (mW)	442.10	458.71	452.33	451.05

Table 2. Results of Left Right Staggered Array

	LR Staggered			
Voltage (V)	4.02	3.83	3.86	3.90
Current (mA)	216.88	205.18	203.34	208.47
Power (mW)	911.21	805.67	797.37	838.08

Table 3. Results of 2-1-2 Array

	2-1-2			
Voltage (V)	3.99	4.05	3.89	3.98
Current (mA)	215.95	214.21	892.03	440.73
Power (mW)	890.27	878.89	933.60	900.92

Table 4. Results of Diagonal Array

	Diagonal			
Voltage (V)	3.77	3.72	3.76	3.75
Current (mA)	200.66	198.77	202.56	200.66
Power (mW)	788.69	776.08	802.43	789.07

Three Turbine Averages, by Array

Table 5. Results of Single File Array

Single File				
Voltage (V)	2.75	2.76	2.75	2.75
Current (mA)	111.96	112.22	111.84	112.00
Power (mW)	455.28	455.78	454.39	455.15
Wind Speed (m/s at 32 Hz)	10.30	10.50	10.35	10.38

Table 6. Results of Left-Right Staggered Array

LR Staggered				
Voltage (V)	3.24	3.19	3.18	3.20
Current (mA)	131.79	130.13	129.67	130.53
Power (mW)	584.83	571.26	567.11	574.40
Wind Speed (m/s at 32 Hz)	10.50	10.60	10.70	10.60

Table 7. Results of 2-1 Array

2-1-2				
Voltage (V)	3.31	3.26	3.26	3.28
Current (mA)	134.94	132.78	132.68	133.47
Power (mW)	603.20	586.02	582.37	590.53
Wind Speed (m/s at 32 Hz)	10.70	10.70	10.80	10.73

Table 8. Results of Diagonal Array

Diagonal				
Voltage (V)	3.14	3.15	3.12	3.14
Current (mA)	128.06	128.15	127.12	127.78
Power (mW)	542.37	546.77	535.23	541.45
Wind Speed (m/s at 32 Hz)	10.80	10.68	10.40	10.63

APPENDIX D

Five Turbine Averages, by Array

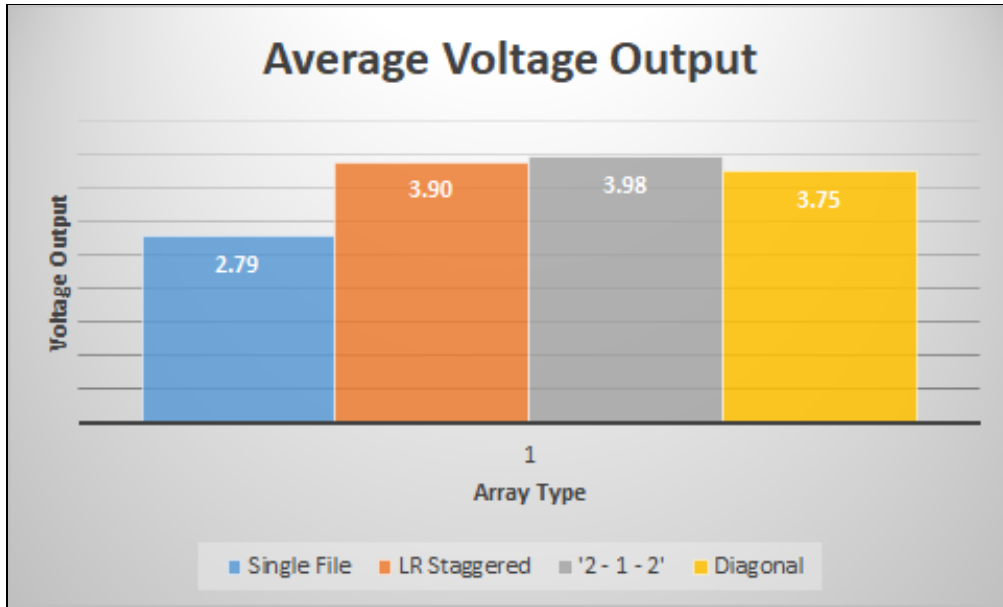


Figure 17: Average Voltage Output

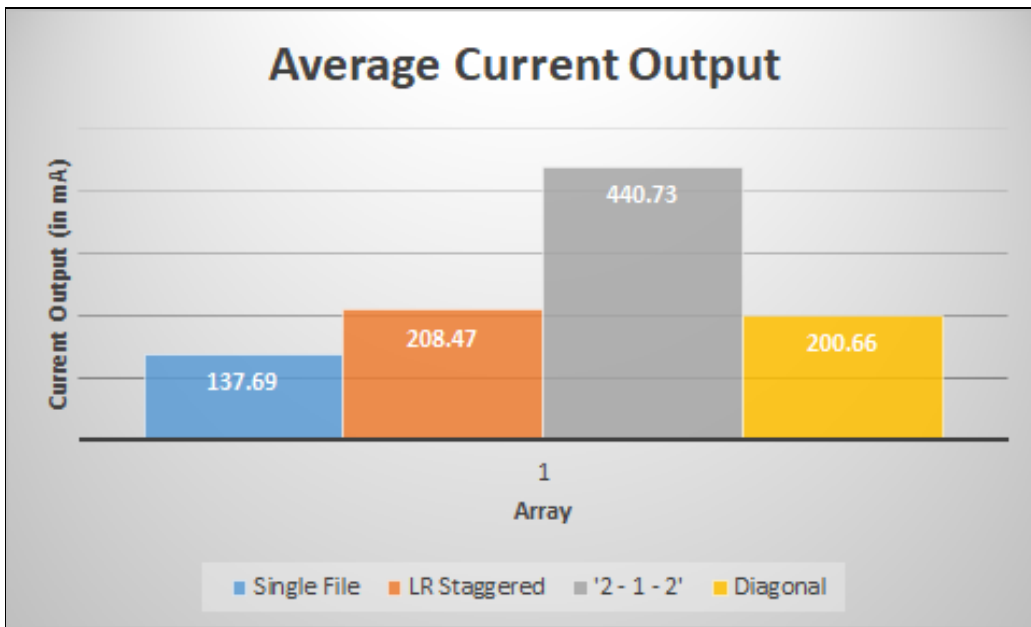


Figure 18: Average Current Output

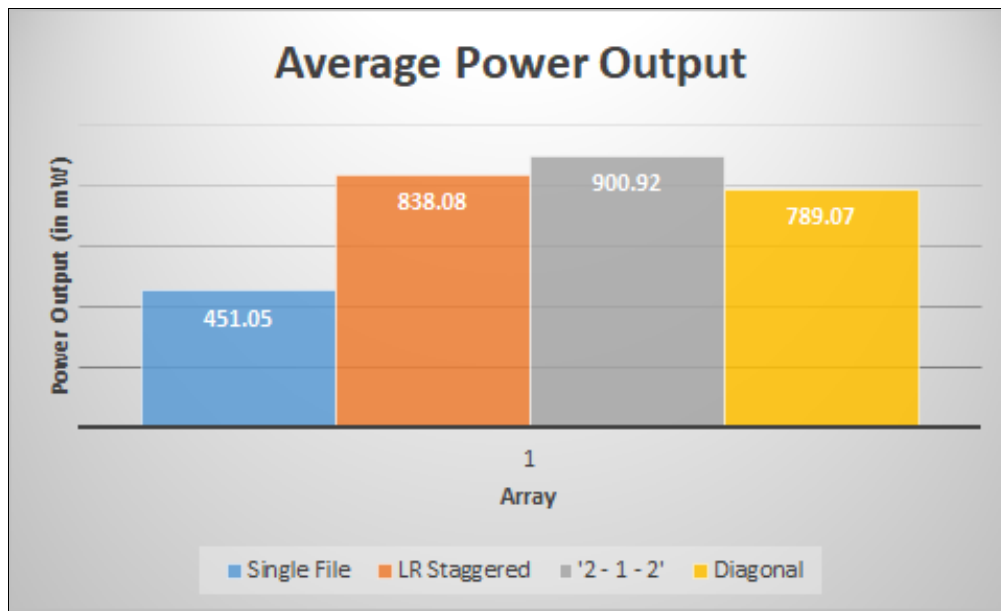


Figure 19: Average Power Output

Three Turbine Averages, by Array

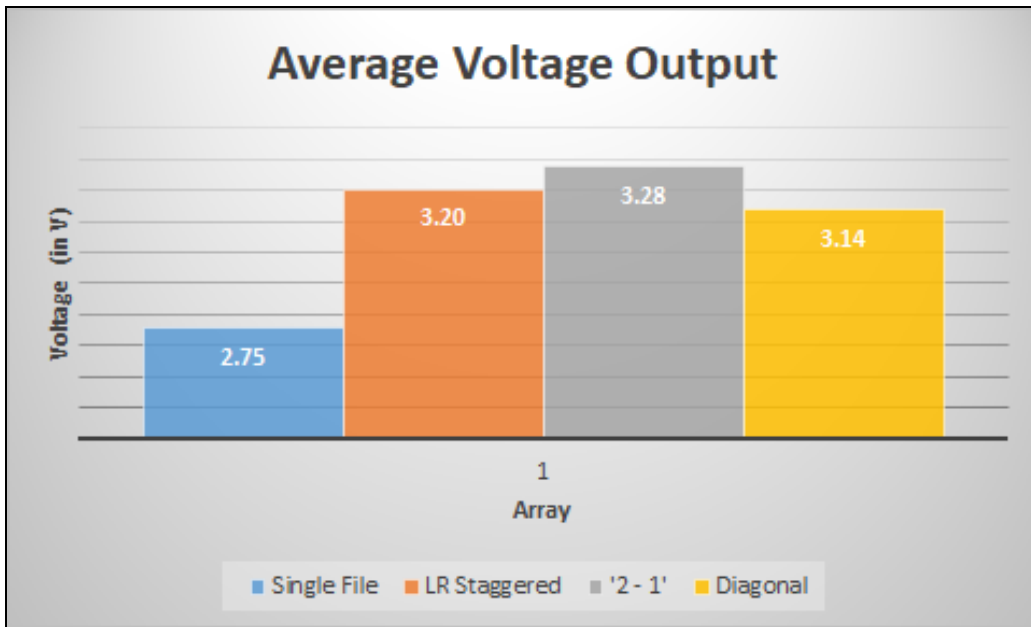


Figure 20: Average Voltage Output

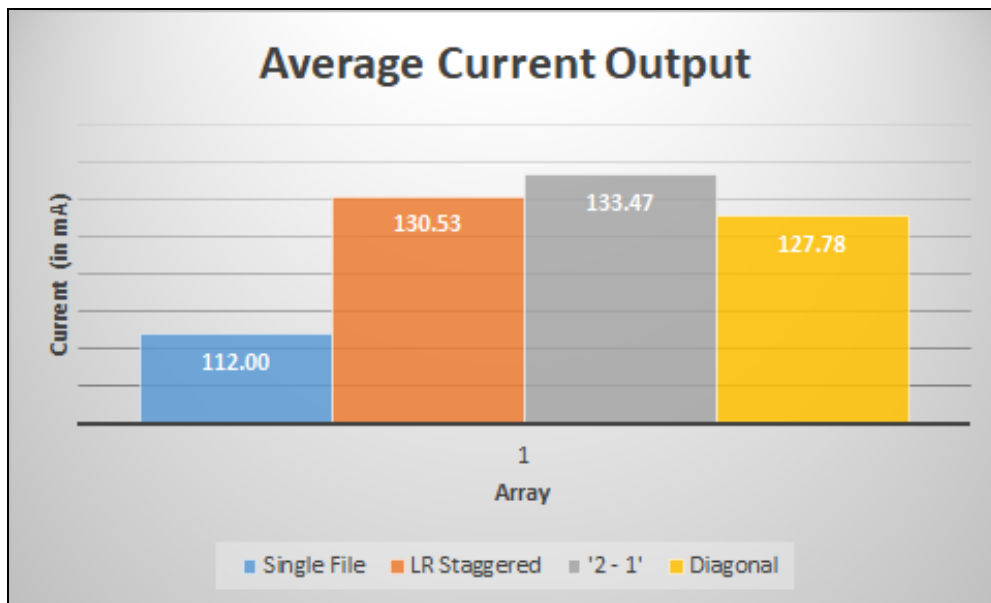


Figure 21: Average Current Output

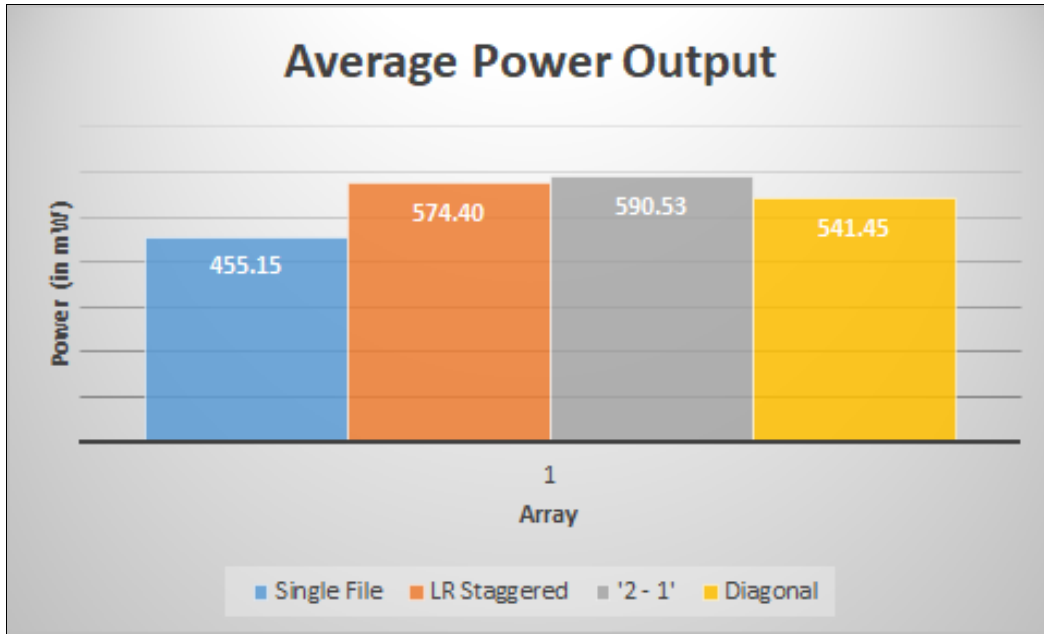


Figure 22: Average Power Output

APPENDIX E

5 Turbine

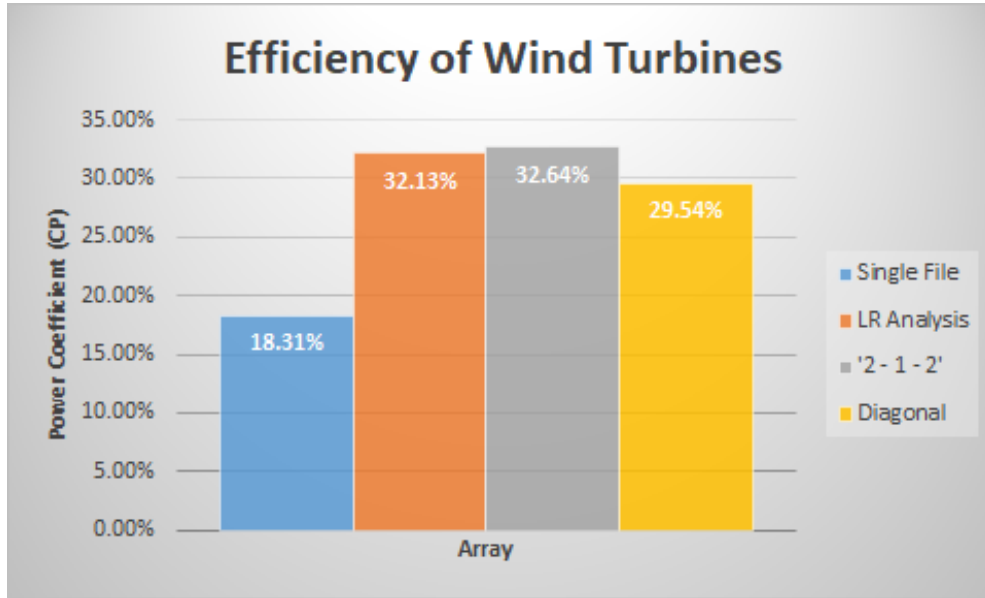


Figure 23: Average Power Coefficient

3 Turbine

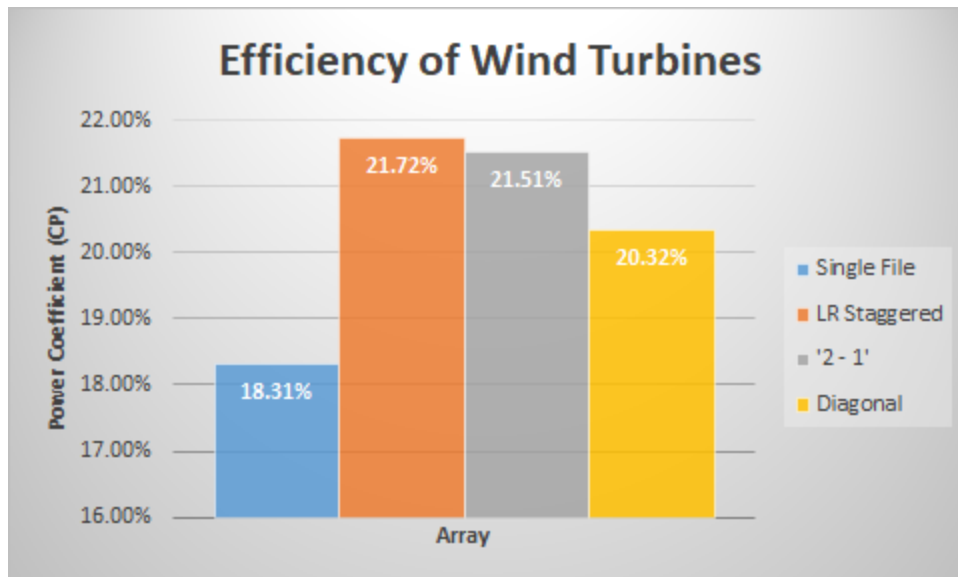


Figure 24: Average Power Coefficient

APPENDIX F

Five Turbine Graphs

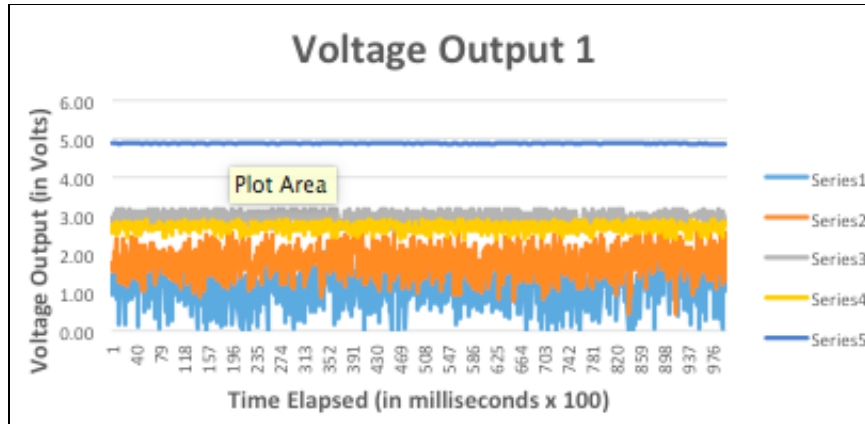


Figure 25. Single File Trial 1

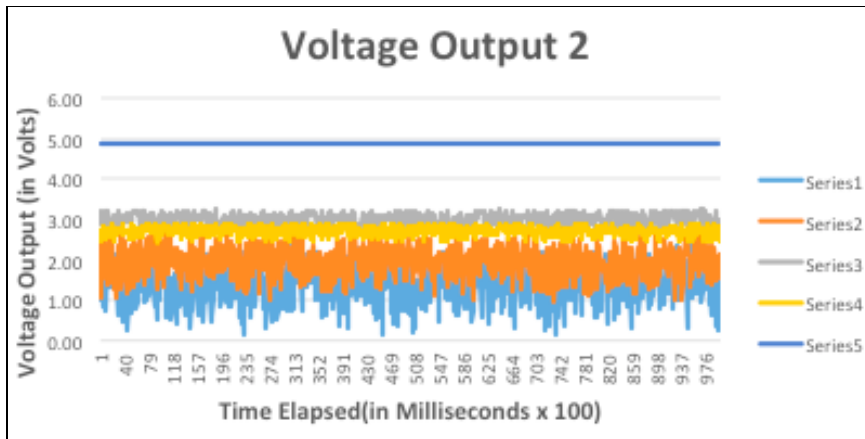


Figure 26. 5 Single File Trial 2

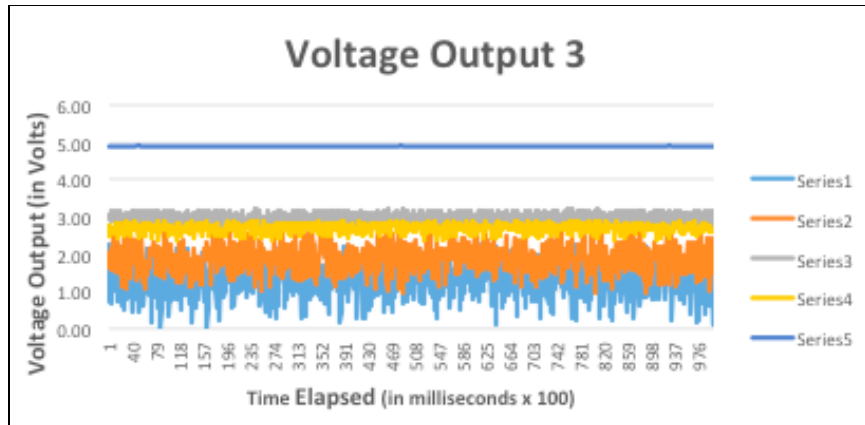


Figure 27. Single File Trial 3

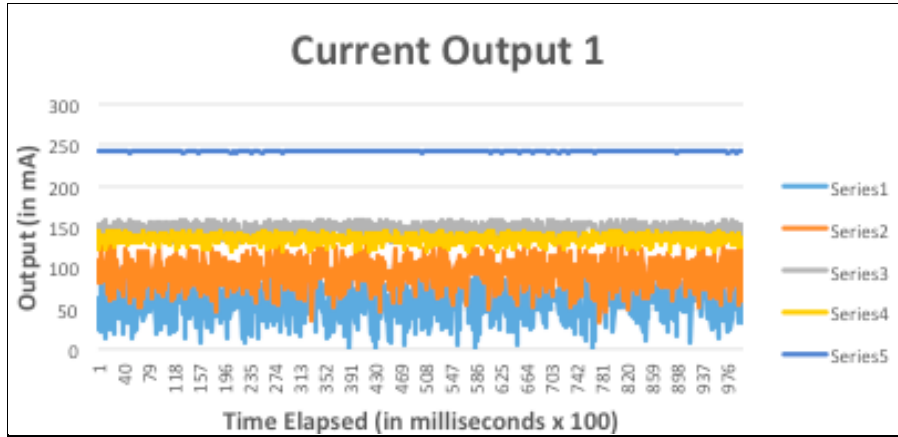


Figure 28. Single File Trial 1

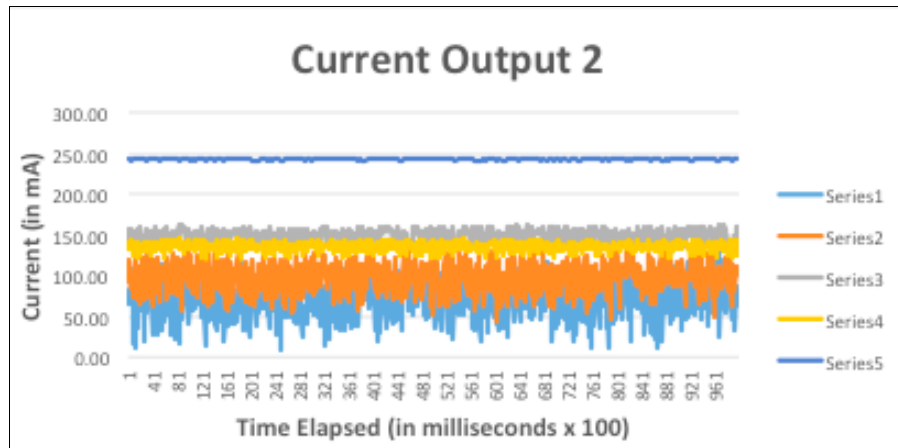


Figure 29. Single File Trial 2

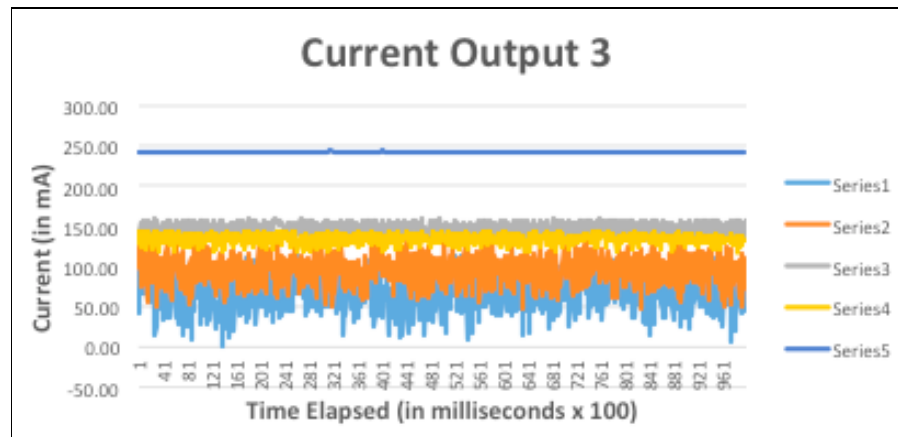


Figure 30. Single File Trial 3

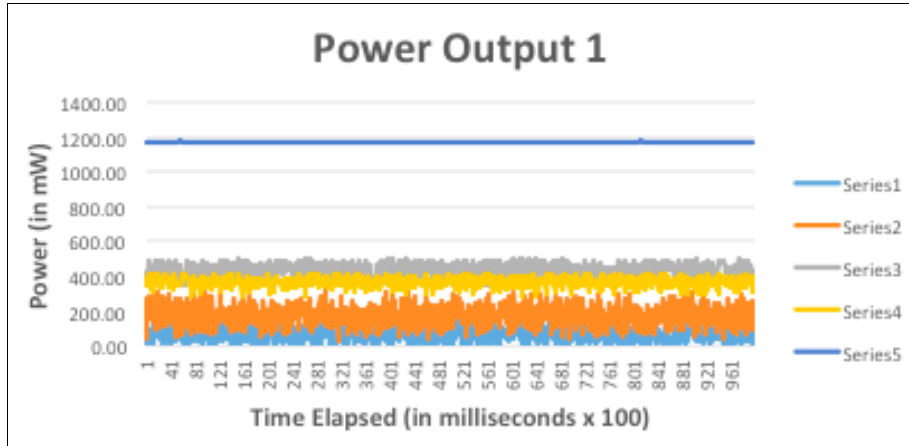


Figure 31 Single File Trial 1

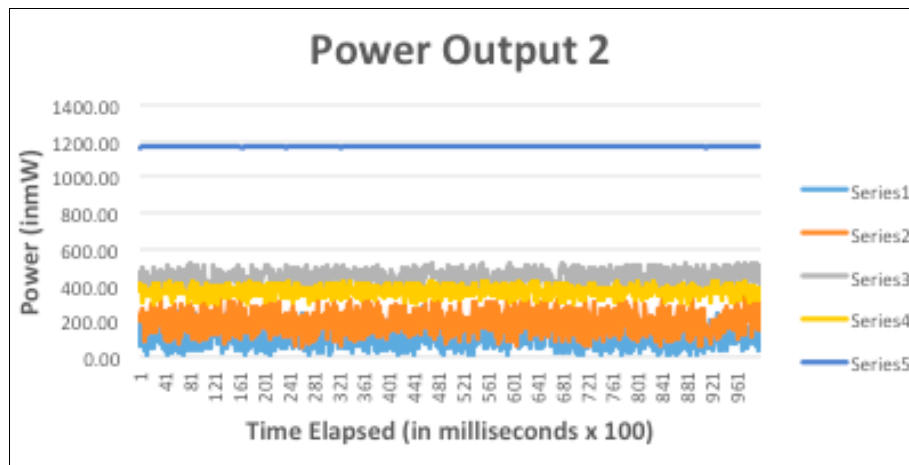


Figure 32. Single File Trial 2

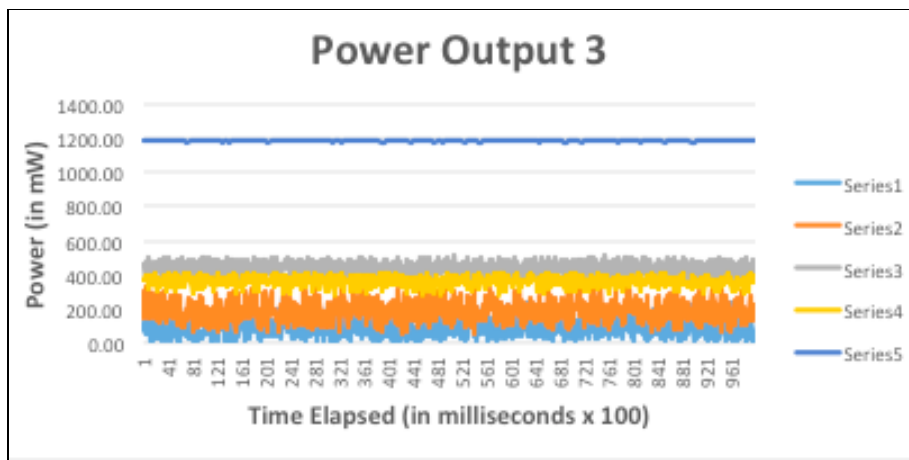


Figure 33. Single File Trial 3

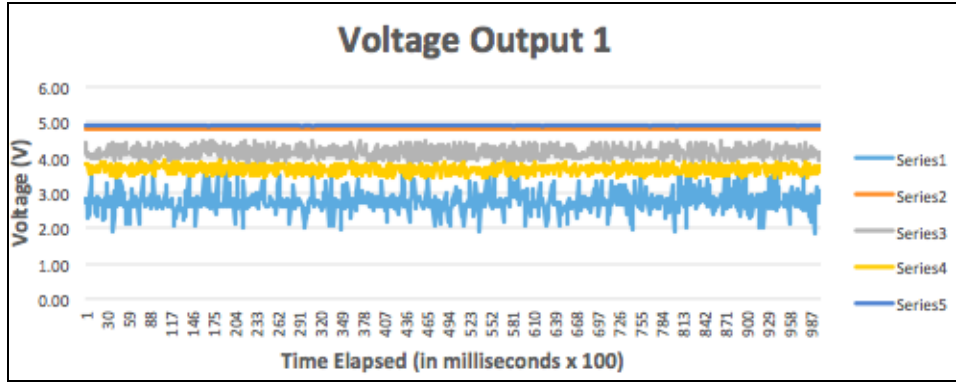


Figure 34. Left-Right Staggered Trial 1

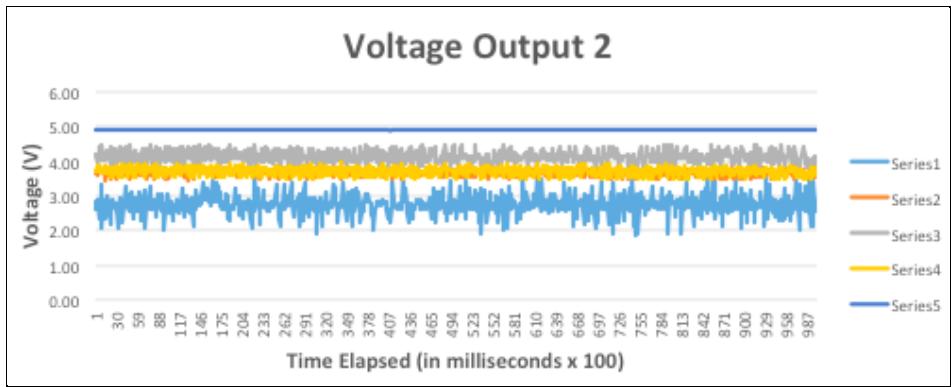


Figure 35. Left-Right Staggered Trial 2

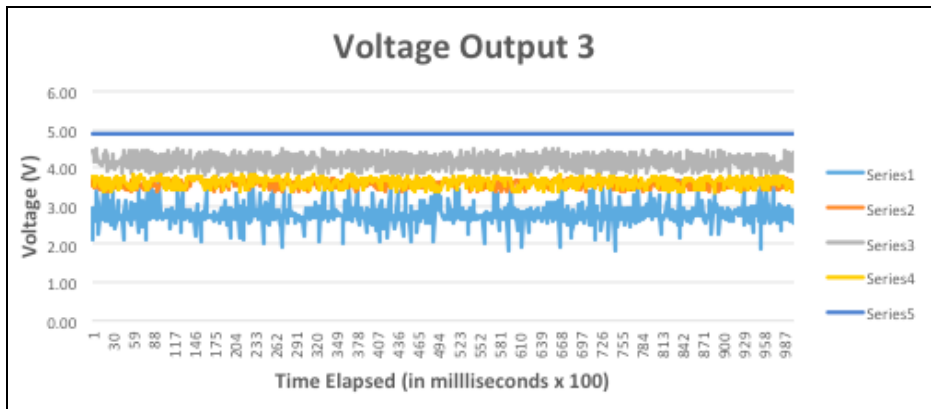


Figure 36. Left-Right Staggered Trial 3

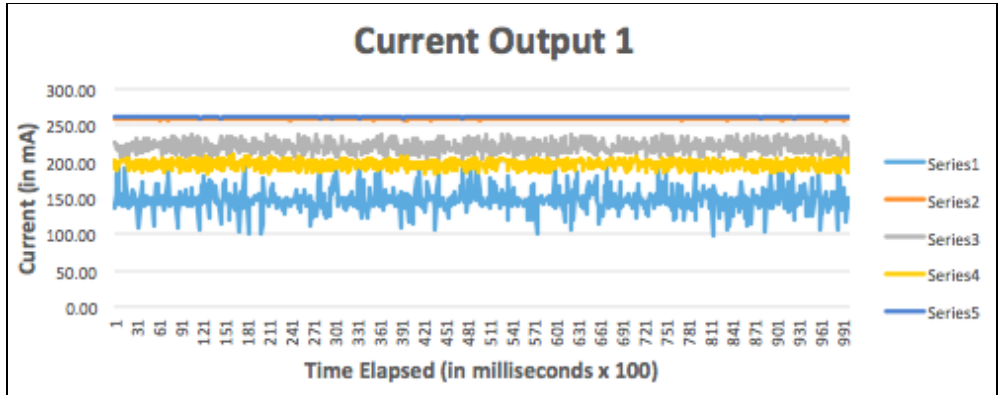


Figure 37. Left-Right Staggered Trial 1

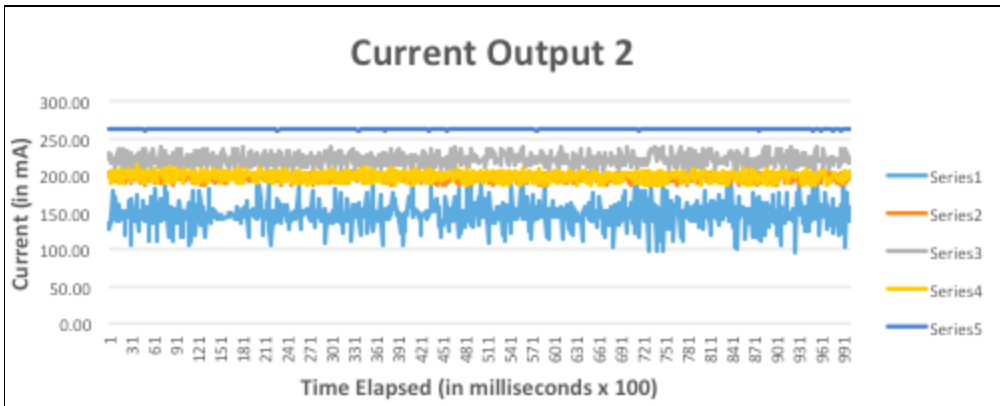


Figure 38. Left-Right Staggered Trial 2

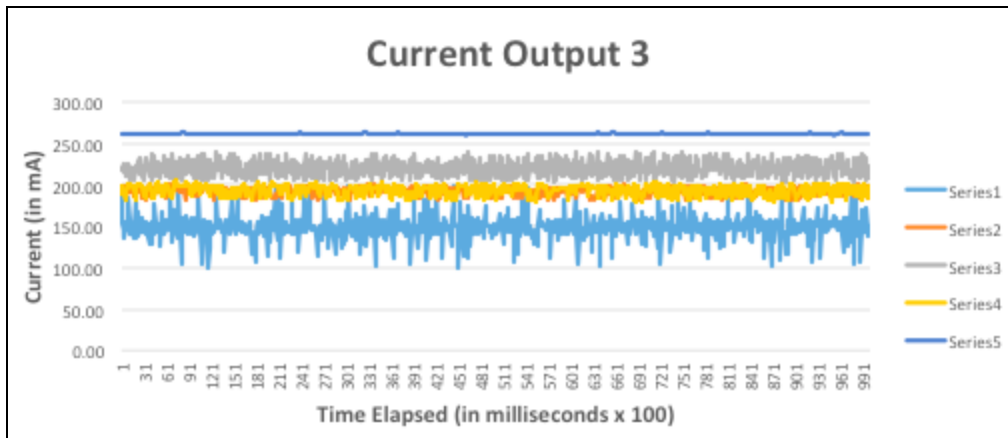


Figure 39. Left-Right Staggered Trial 3

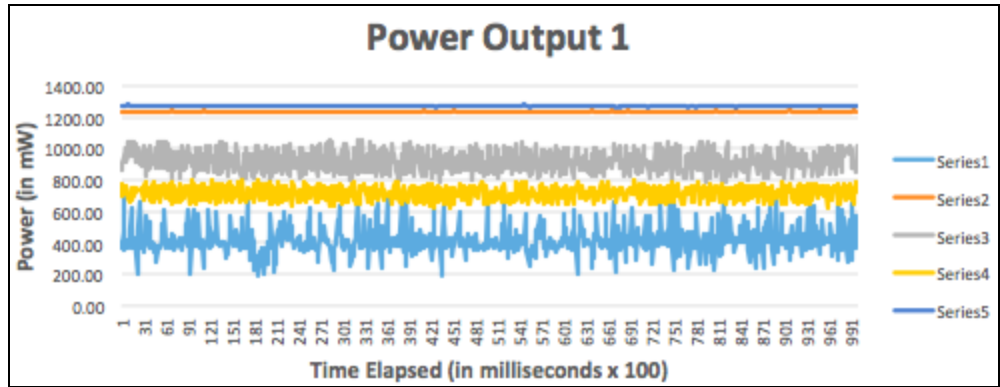


Figure 40. Left-Right Staggered Trial 1

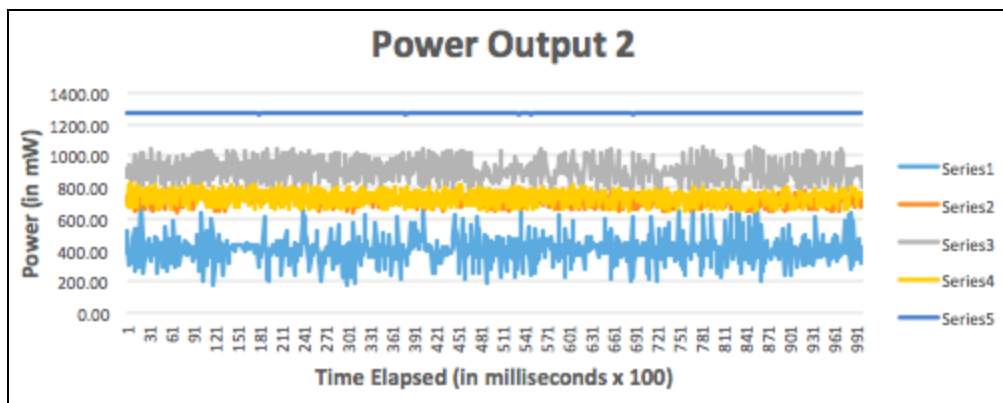


Figure 41. Left-Right Staggered Trial 2

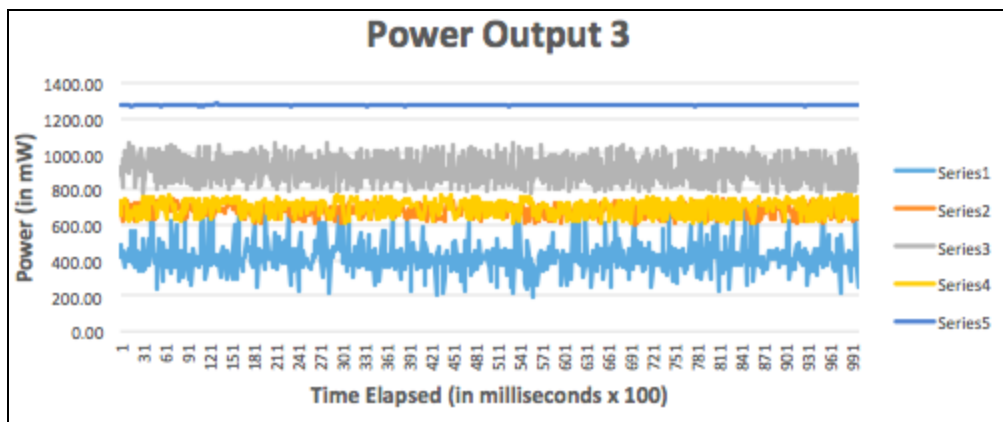


Figure 42. Left-Right Staggered Trial 3

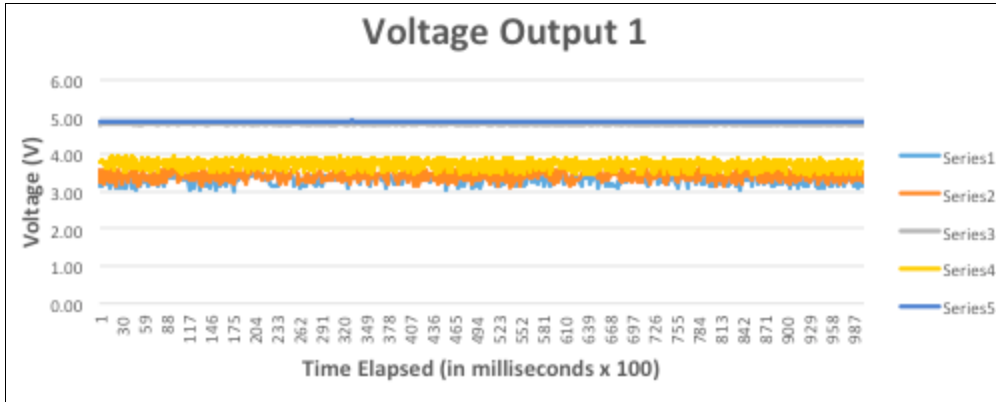


Figure 43. 2-1-2 Trial 1

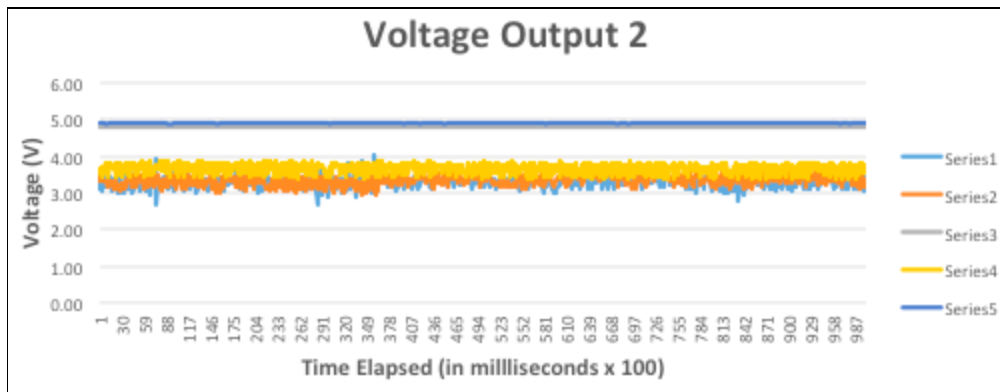


Figure 44. 2-1-2 Trial 2

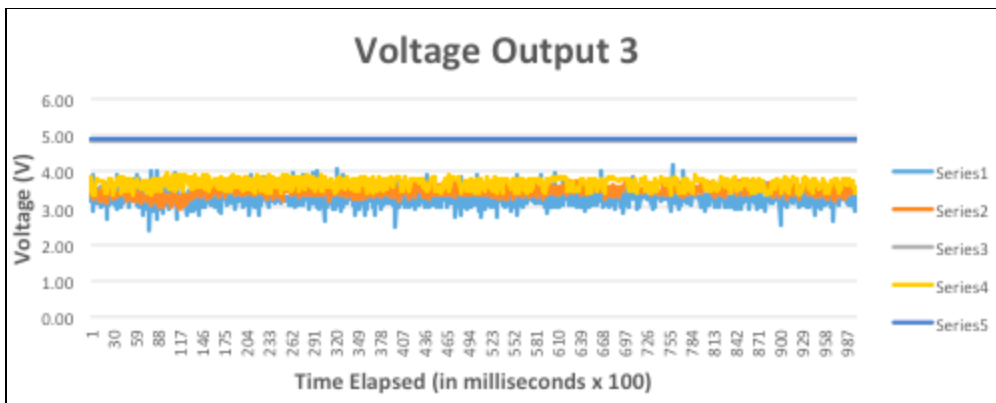


Figure 45. 2-1-2 Trial 3

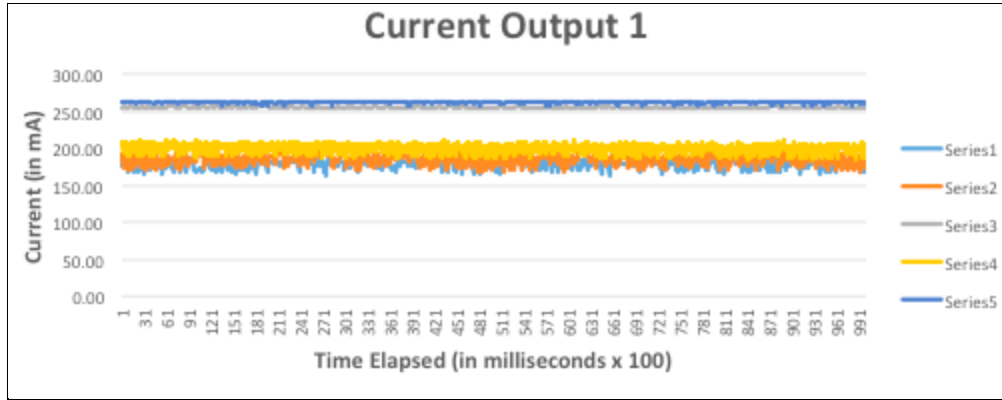


Figure 46. 2-1-2 Trial 1

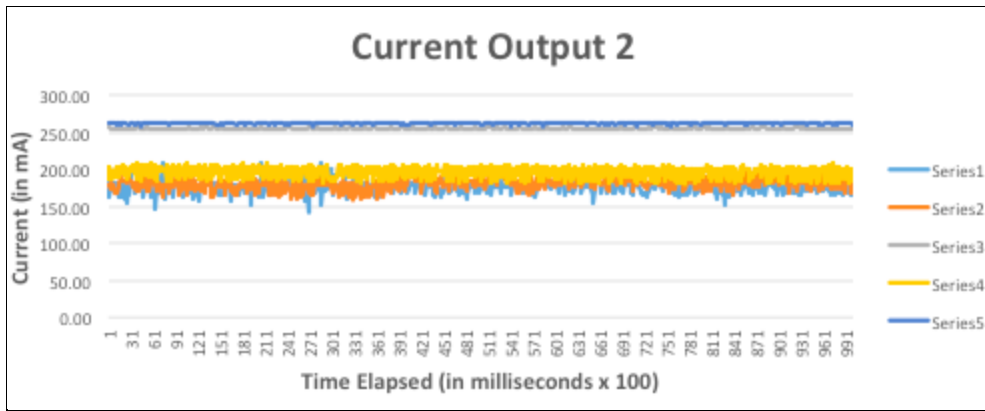


Figure 47. 2-1-2 Trial 2

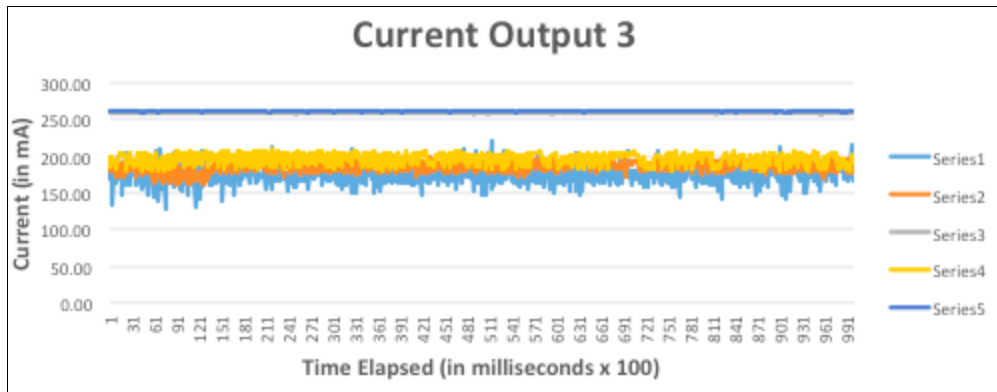


Figure 48. 2-1-2 Trial 3

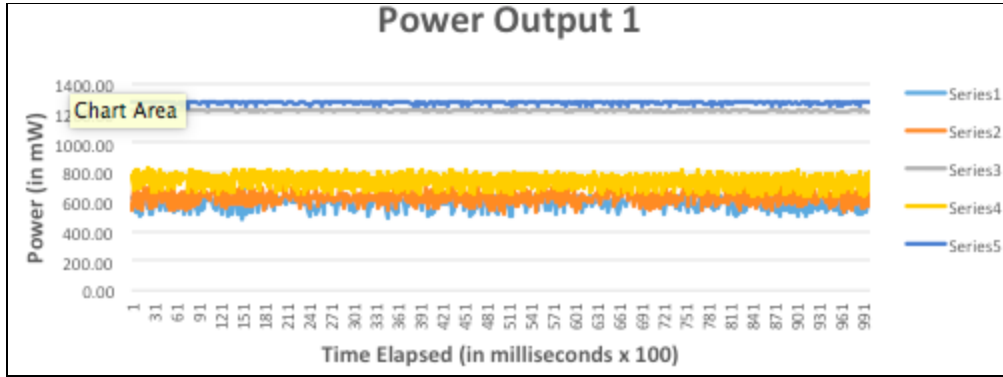


Figure 49. 2-1-2 Trial 1

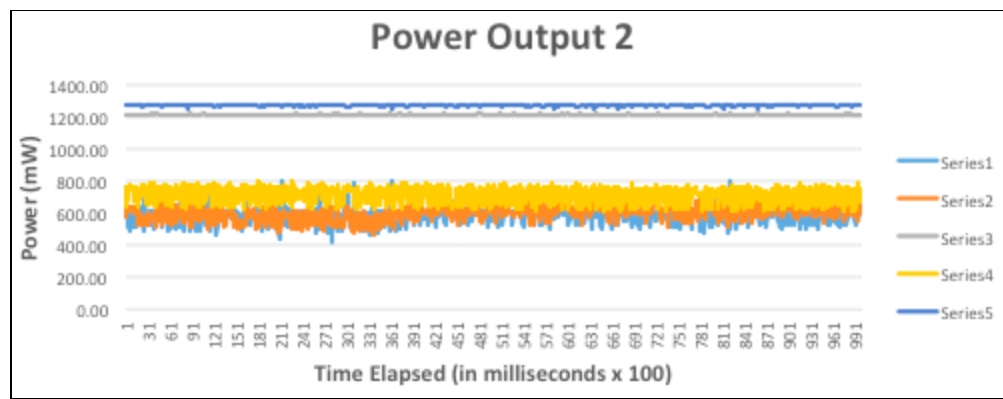


Figure 50. 2-1-2 Trial 2

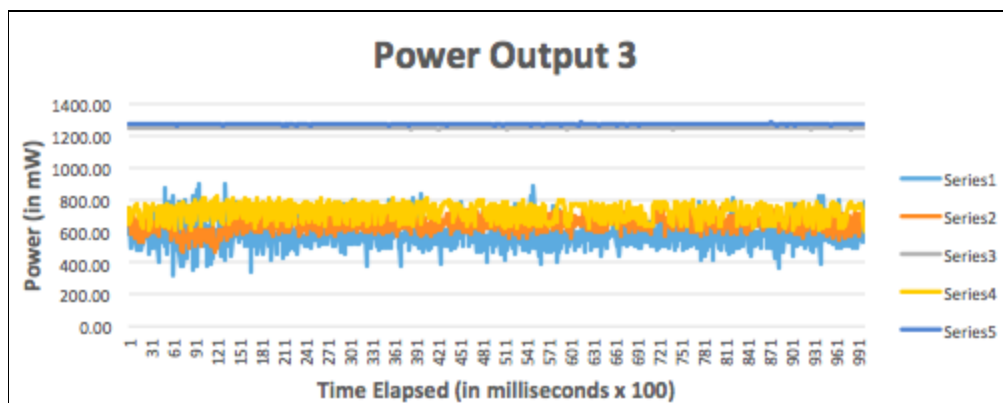


Figure 51. 2-1-2 Trial 3

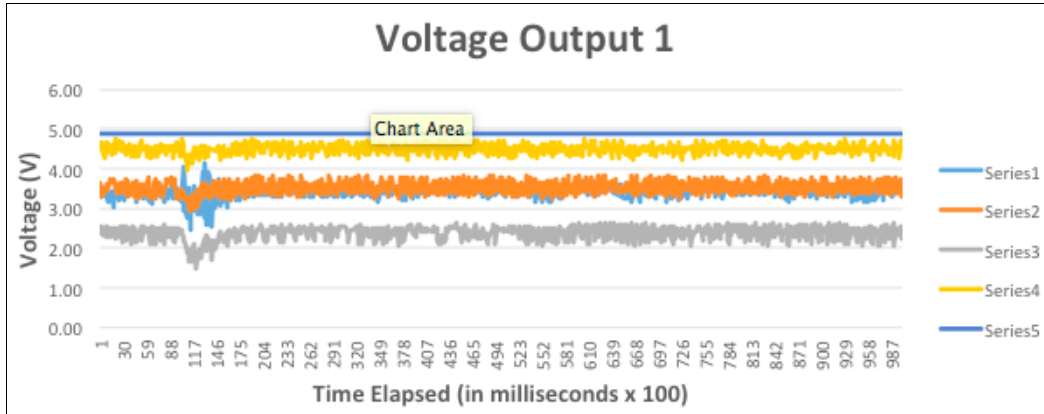


Figure 52. Diagonal Trial 1

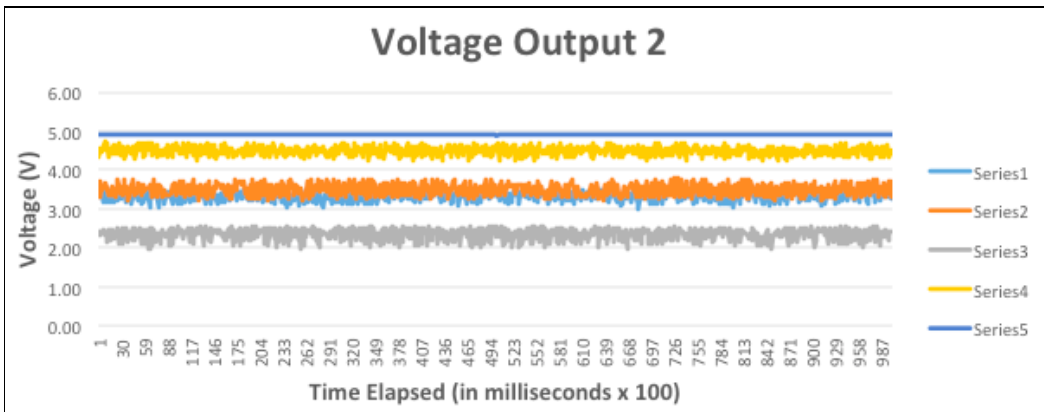


Figure 53. Diagonal Trial 2

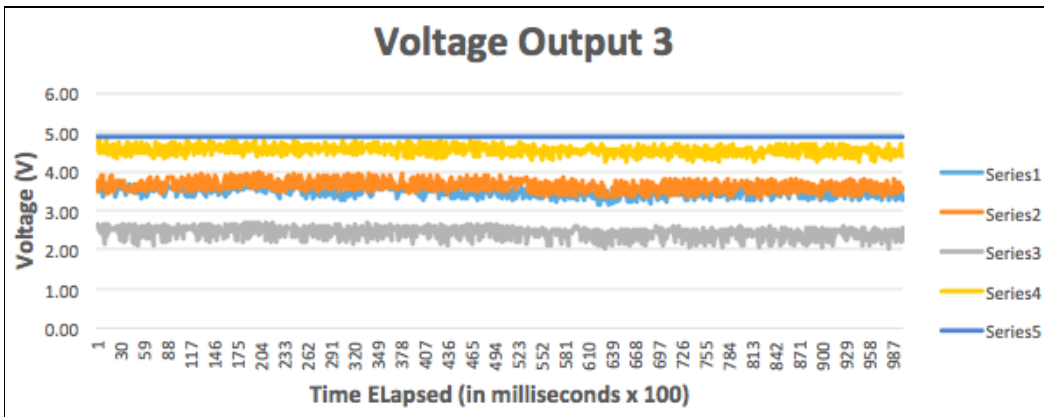


Figure 54. Diagonal Trial 3

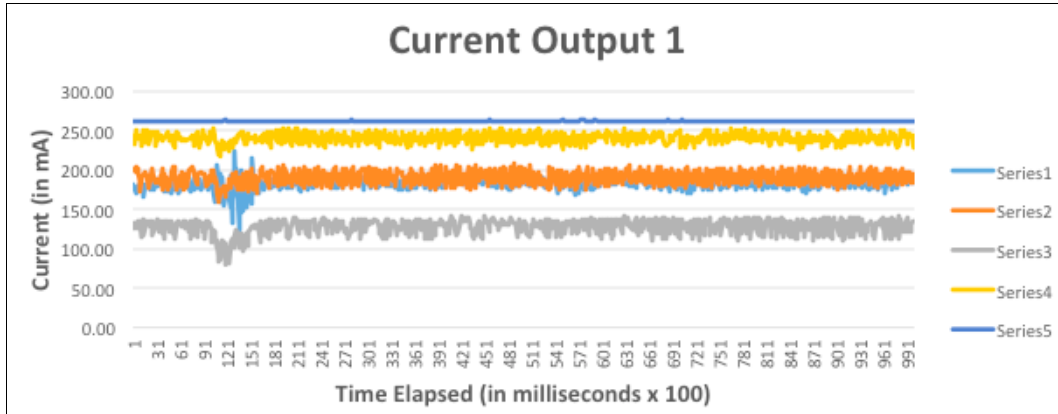


Figure 55. Diagonal Trial 1

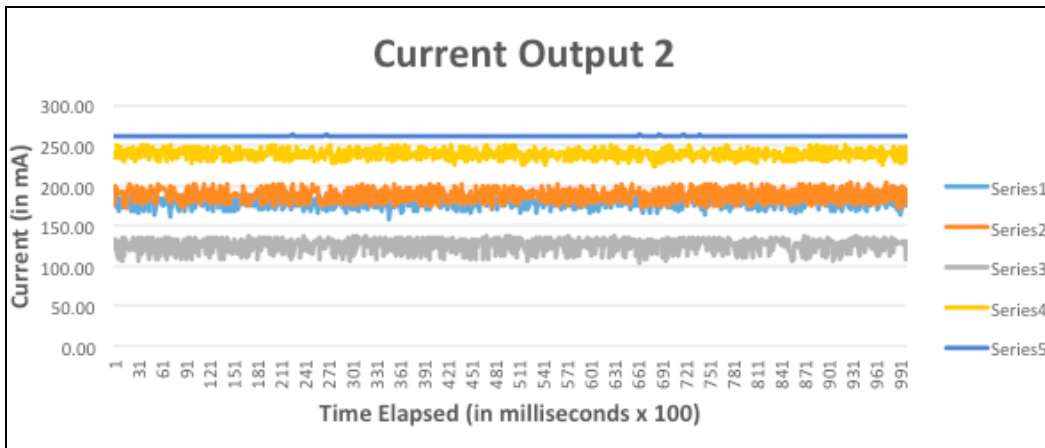


Figure 56. Diagonal Trial 2

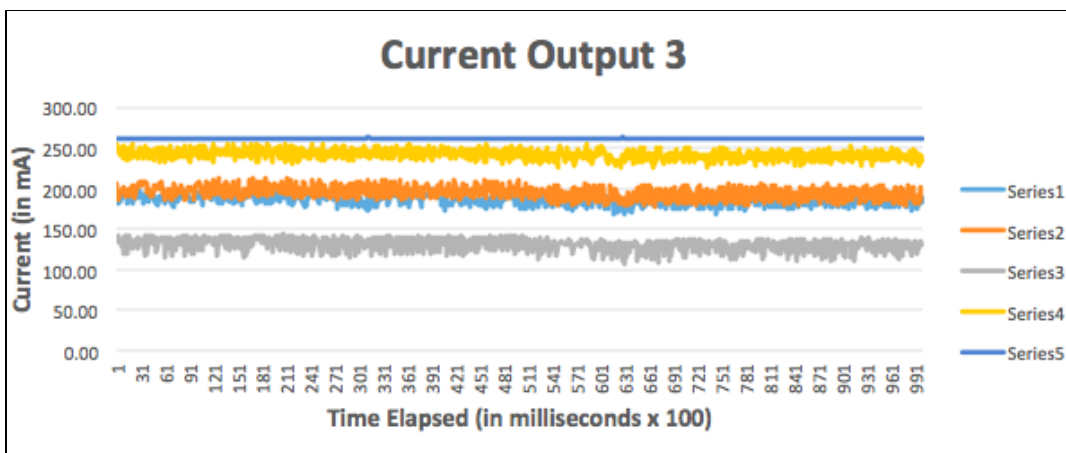


Figure 57. Diagonal Trial 3

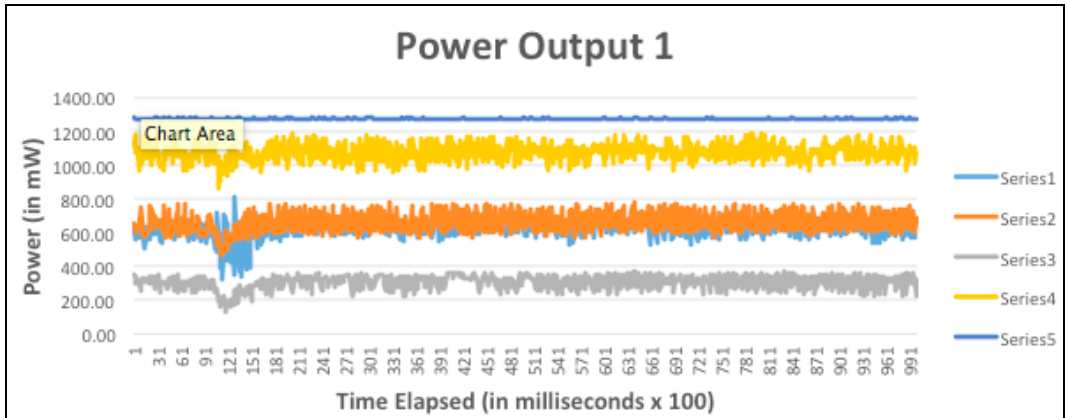


Figure 58. Diagonal Trial 1

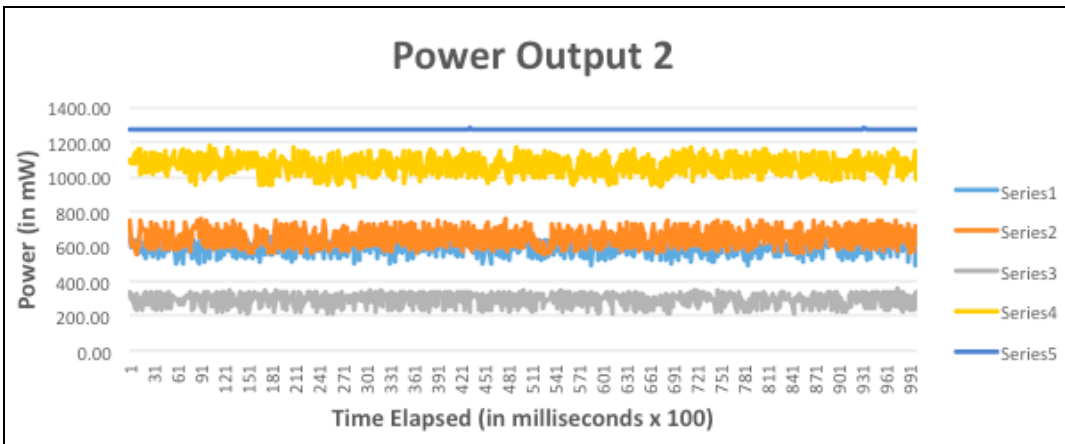


Figure 59. Diagonal Trial 2

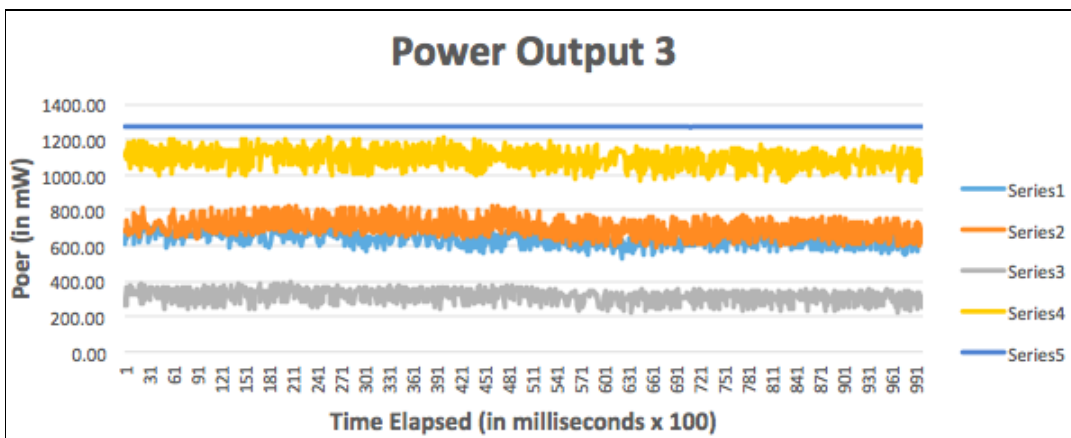


Figure 60. Diagonal Trial 3

APPENDIX G

Three Turbine Graphs

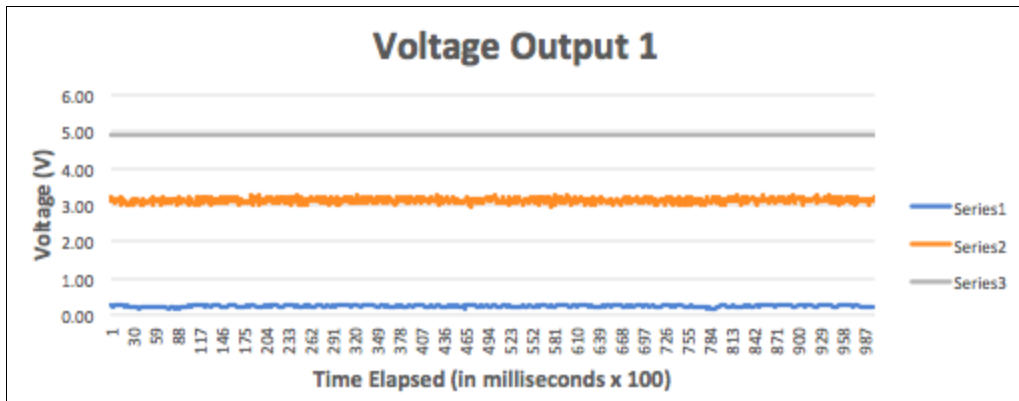


Figure 61. Single File Trial 1

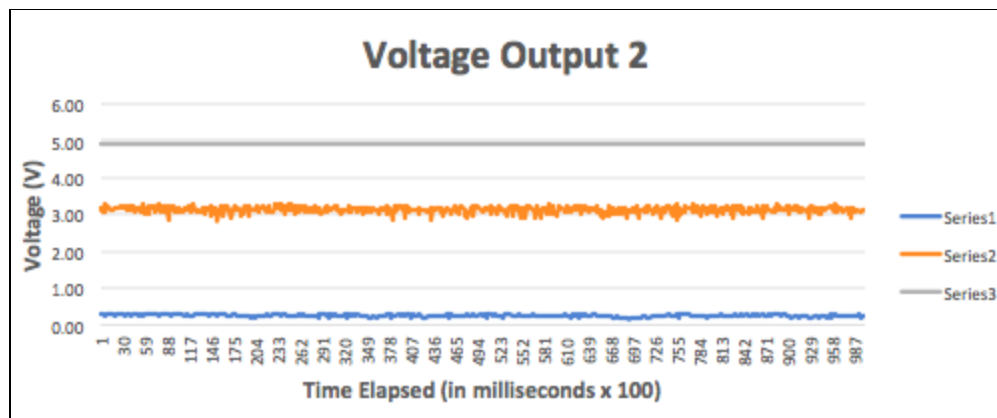


Figure 61. Single File Trial 2

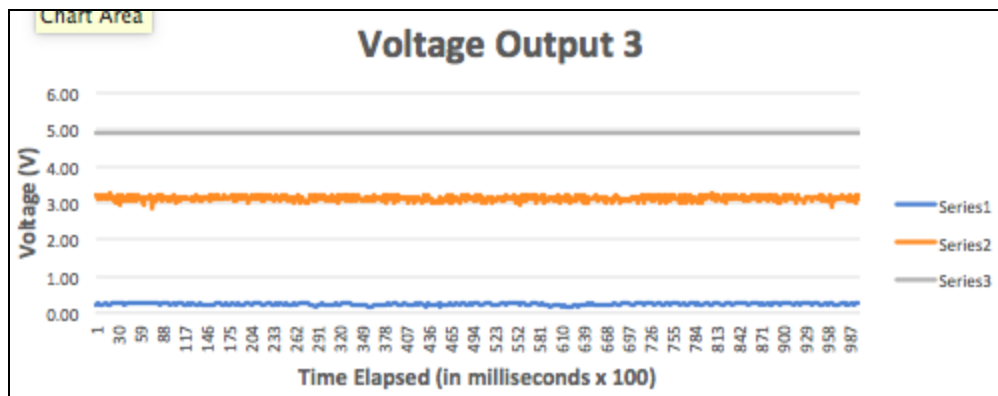


Figure 62. Single File Trial 3

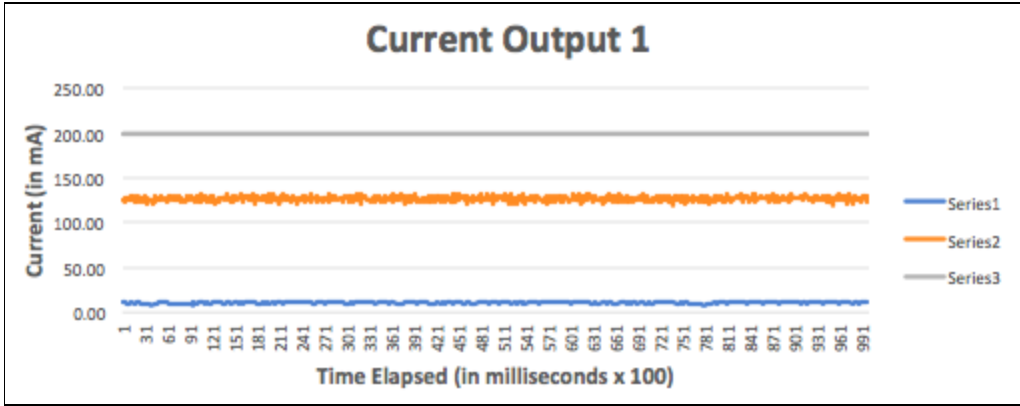


Figure 63. Single File Trial 1

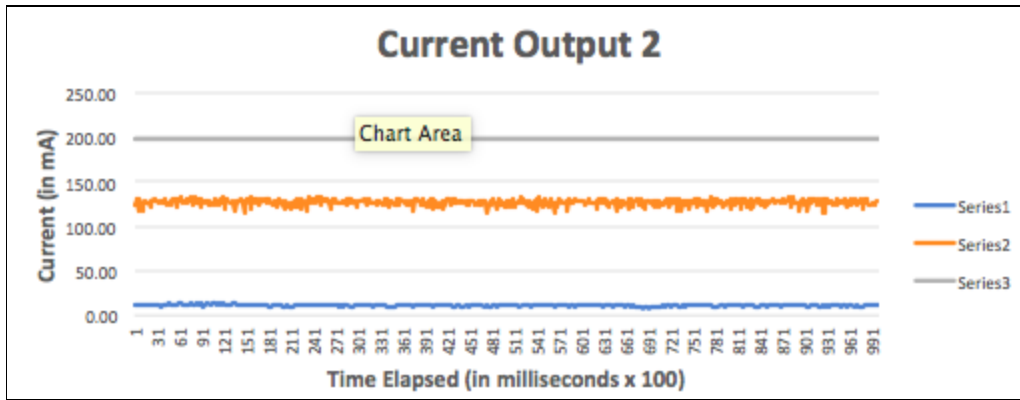


Figure 64. Single File Trial 2

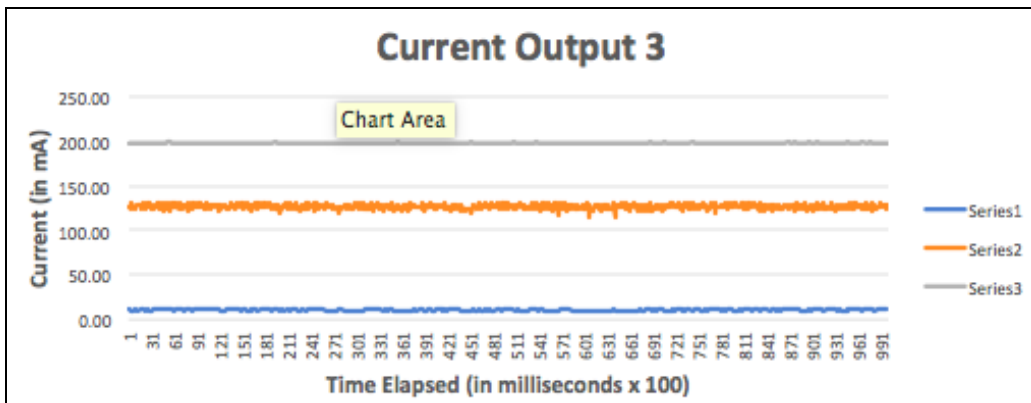


Figure 65. Single File Trial 3

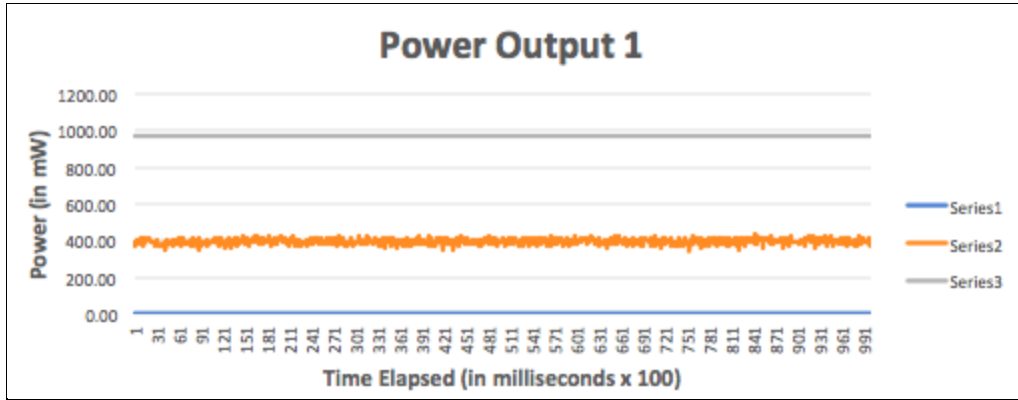


Figure 66. Single File Trial 1

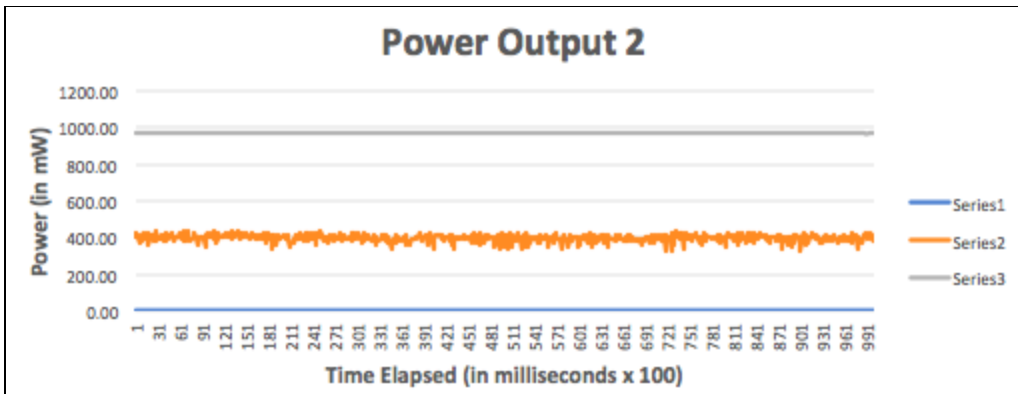


Figure 67. Single File Trial 2

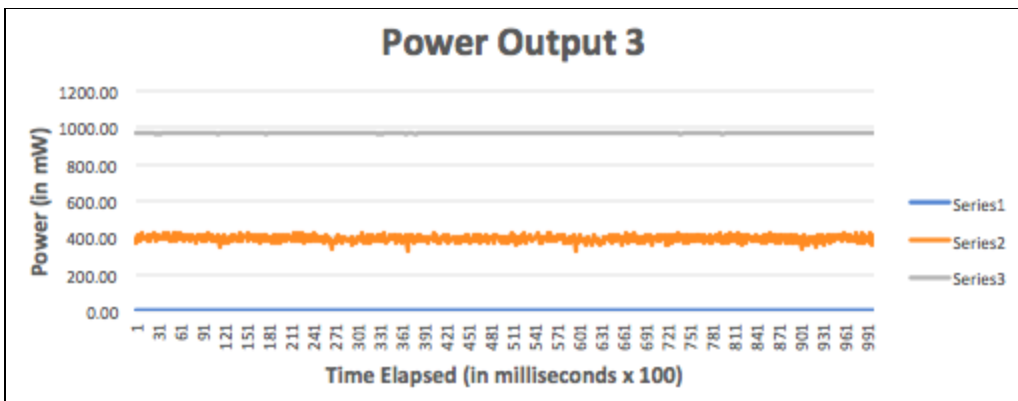


Figure 68. Single File Trial 3

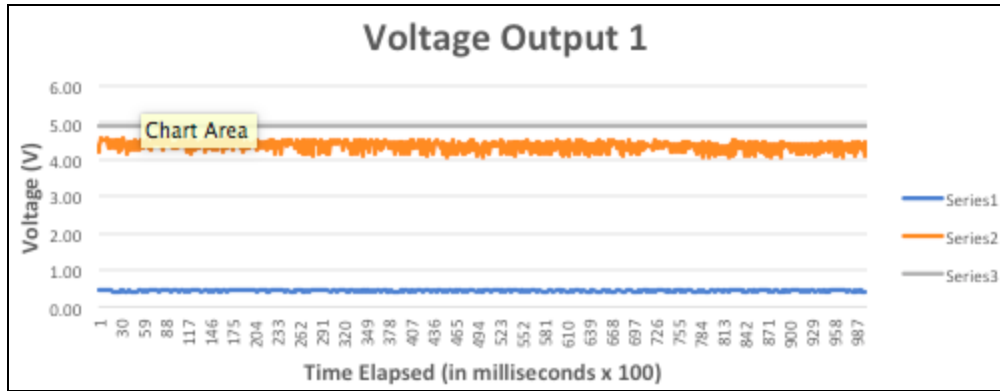


Figure 69. Left-Right Staggered Trial 1

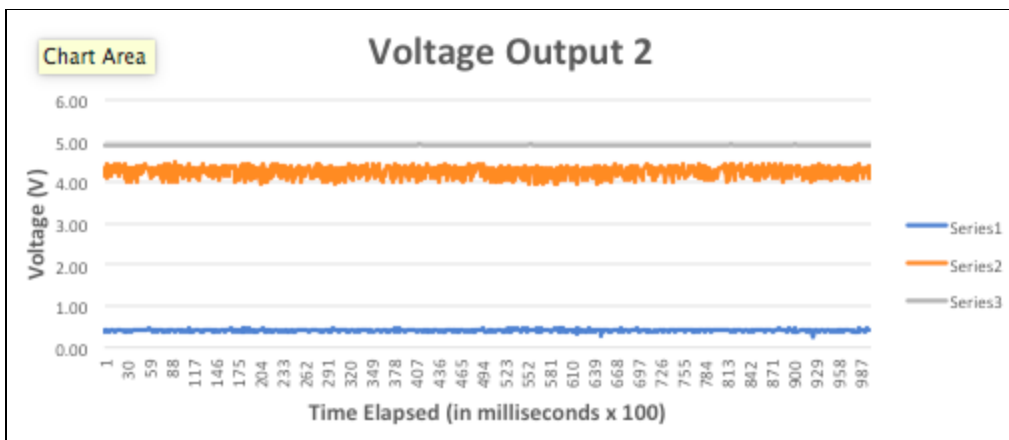


Figure 70. Left-Right Staggered Trial 2

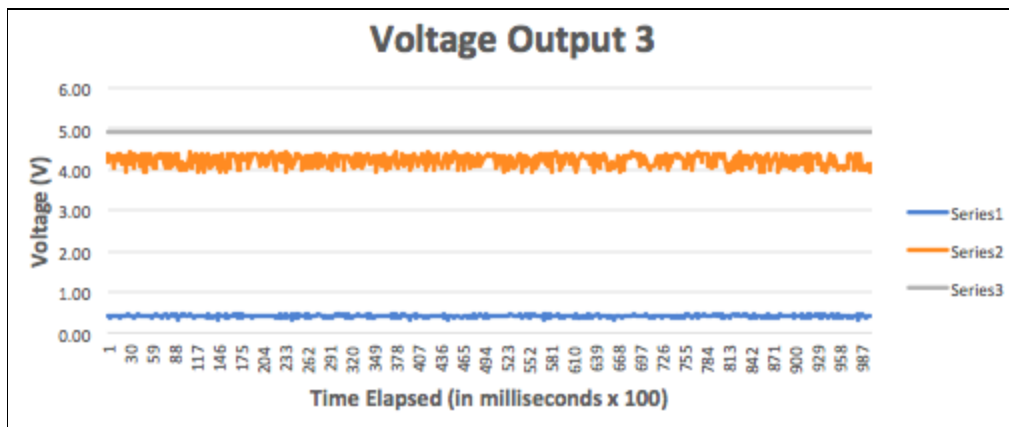


Figure 71. Left-Right Staggered Trial 3

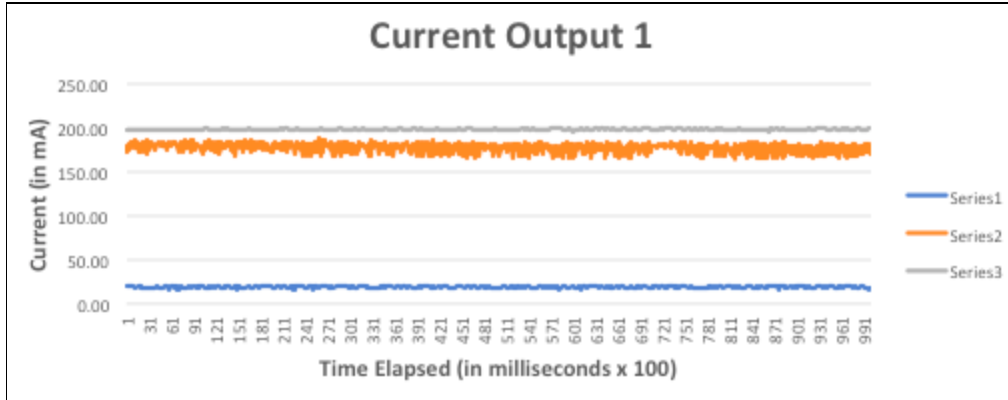


Figure 72. Left-Right Staggered Trial 1

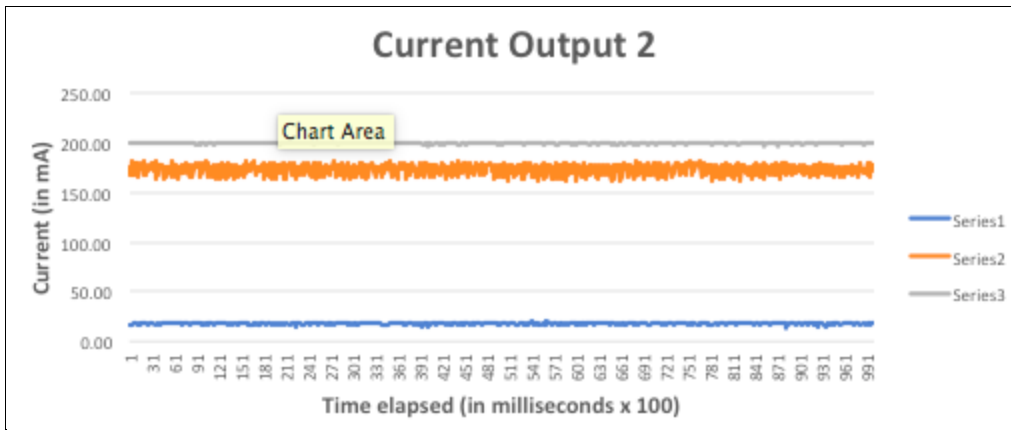


Figure 73. Left-Right Staggered Trial 2

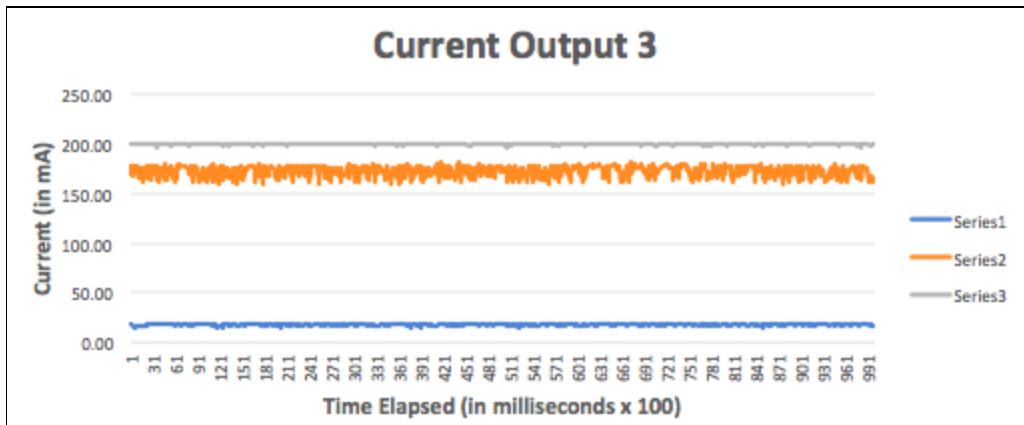


Figure 74. Left-Right Staggered Trial 3

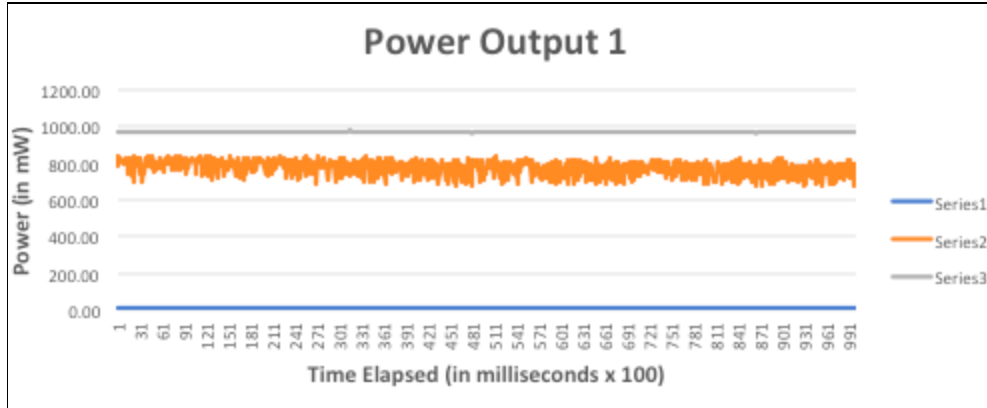


Figure 75. Left-Right Staggered Trial 1

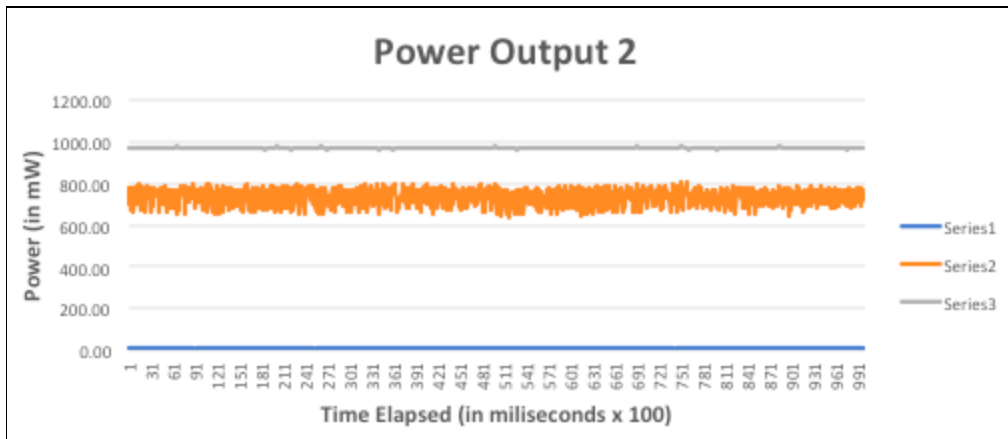


Figure 76. Left-Right Staggered Trial 2

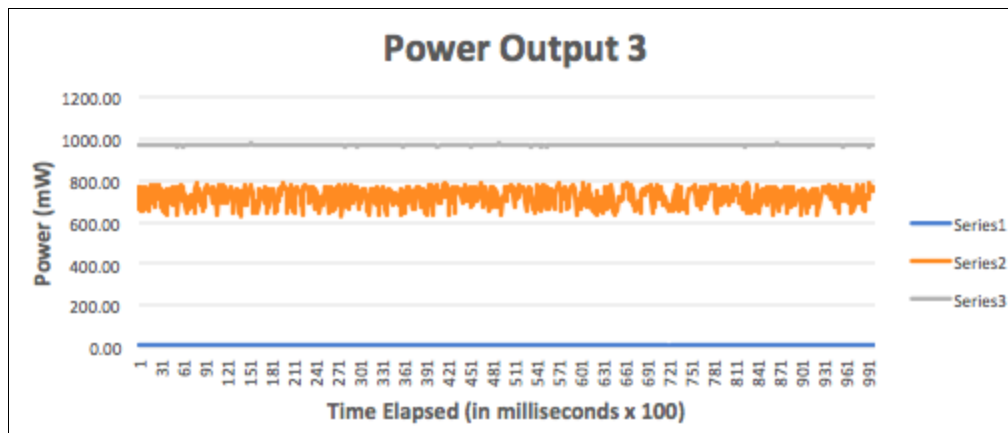


Figure 77. Left-Right Staggered Trial 3

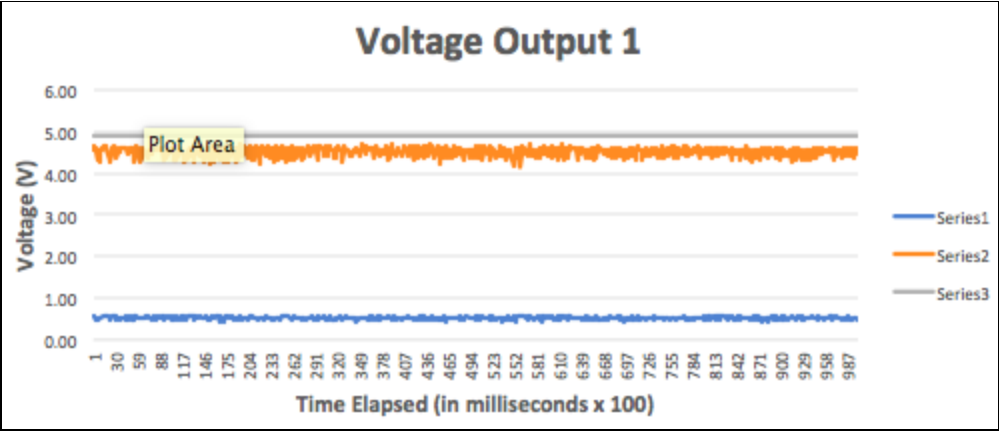


Figure 78. 2-1 Trial 1

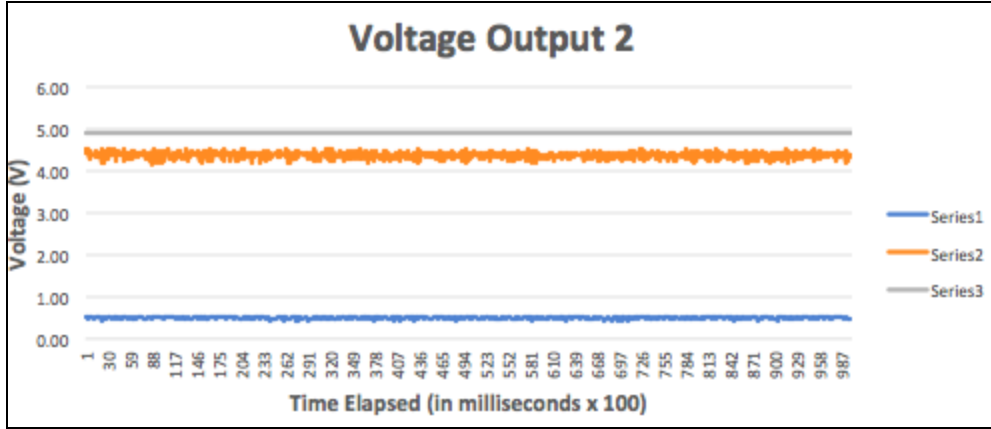


Figure 79. 2-1 Trial 2

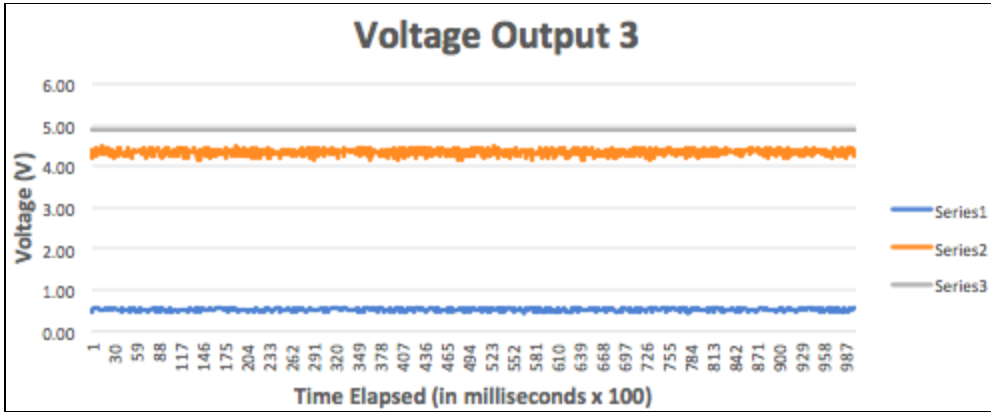


Figure 80. 2-1 Trial 3

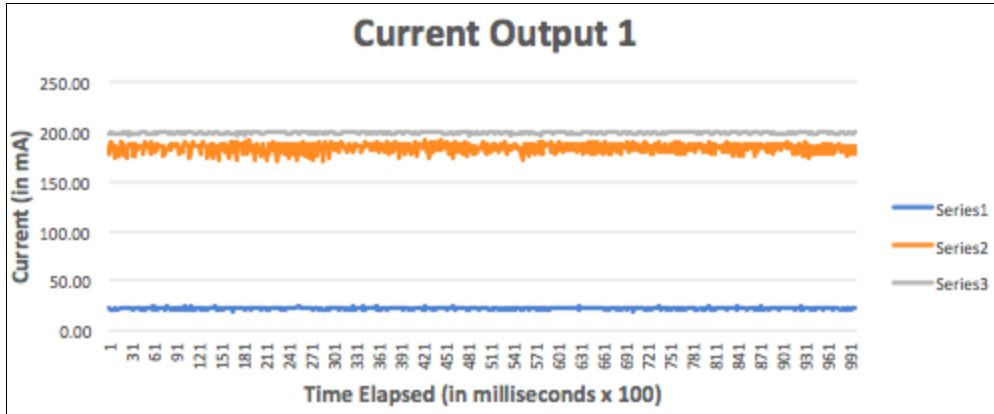


Figure 81. 2-1 Trial 1

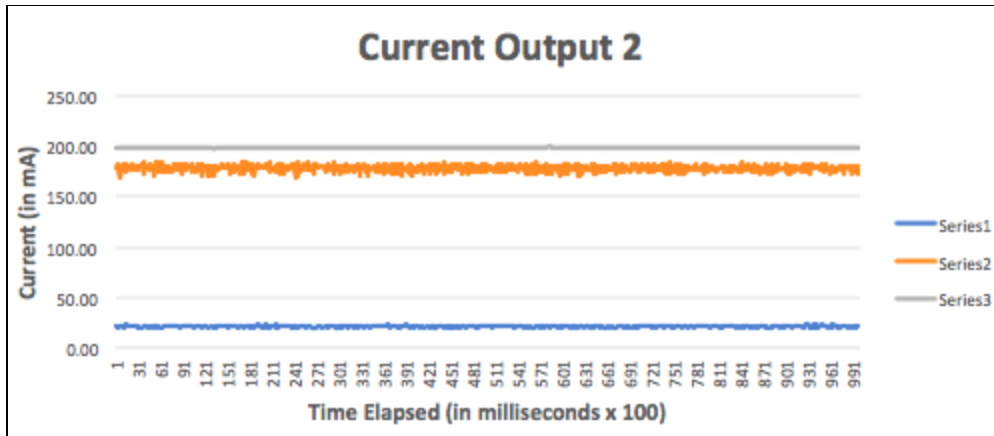


Figure 82. 2-1 Trial 2

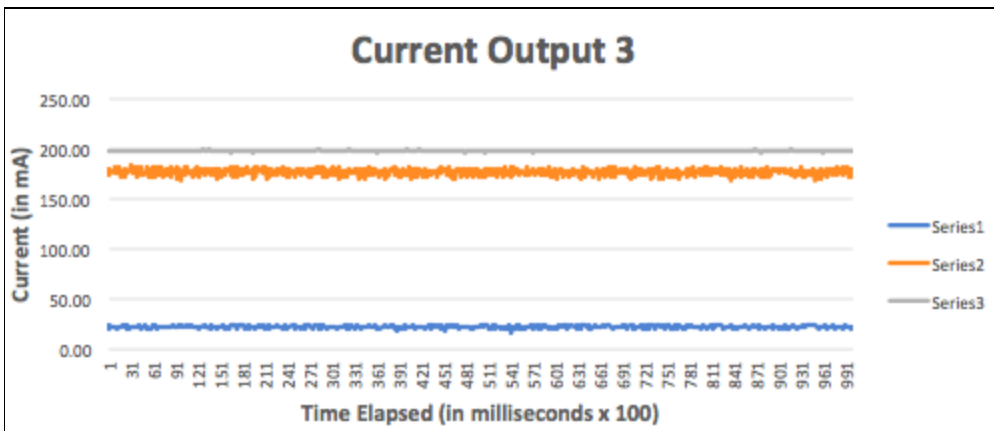


Figure 83. 2-1 Trial 3

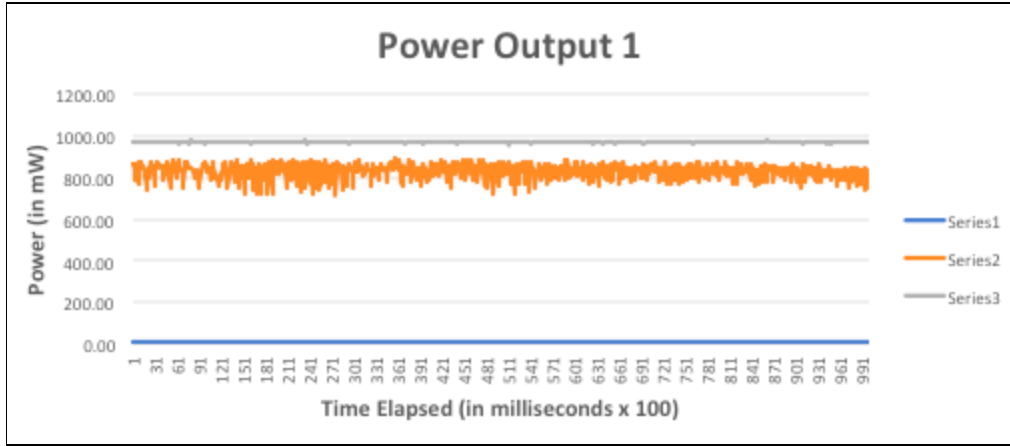


Figure 84. 2-1 Trial 1

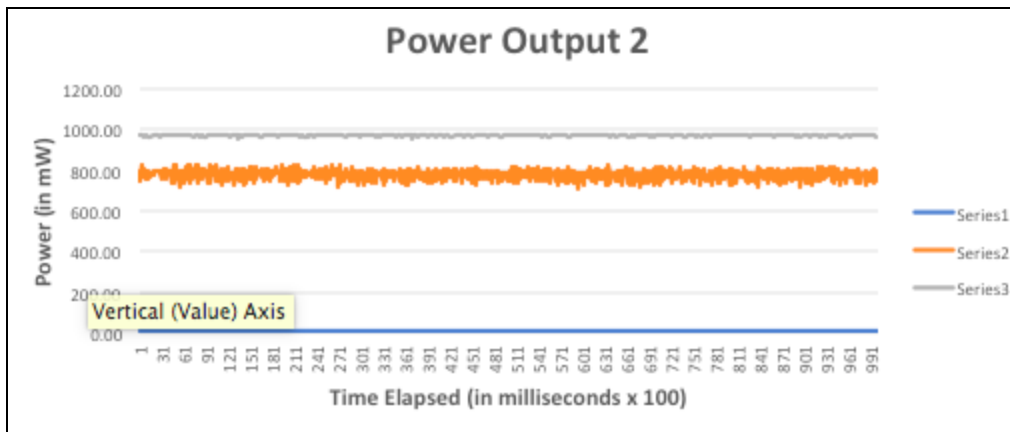


Figure 85. 2-1 Trial 2



Figure 86. 2-1 Trial 3

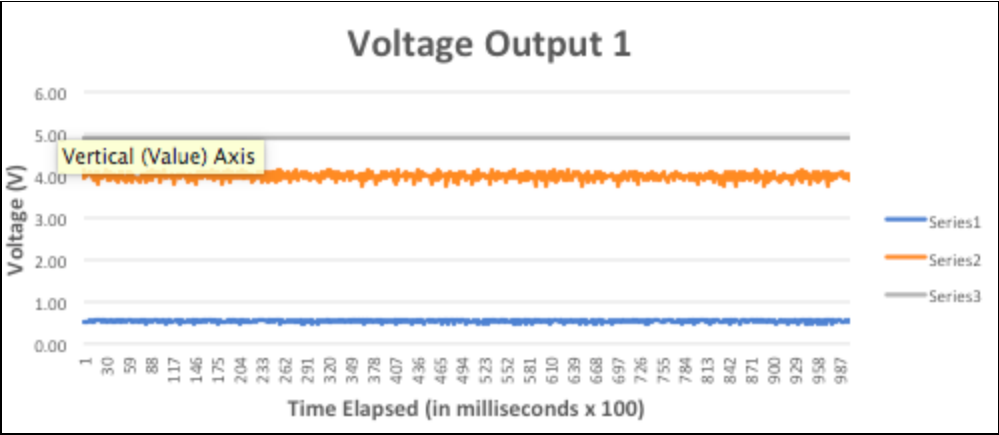


Figure 87. Diagonal Trial 1

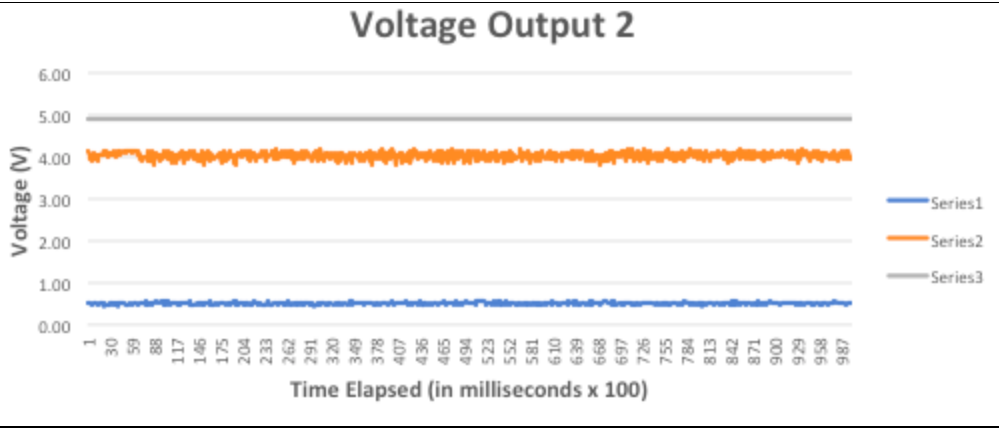


Figure 88. Diagonal Trial 2

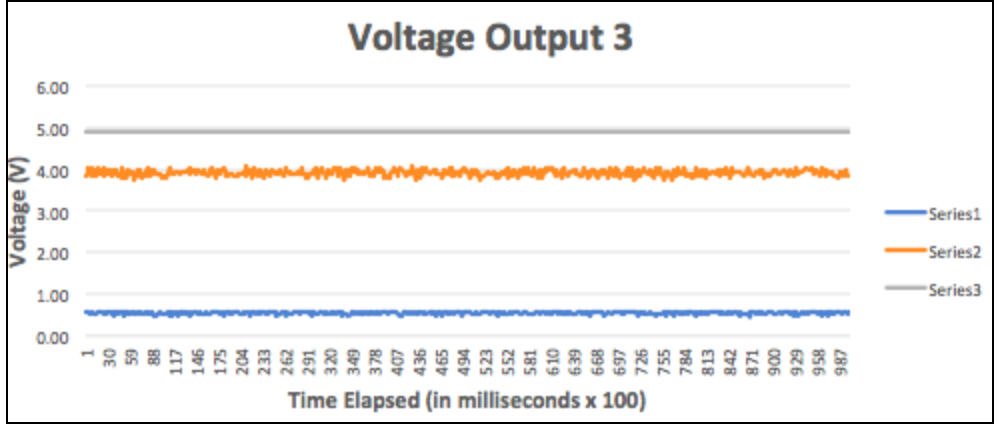


Figure 89. Diagonal Trial 3

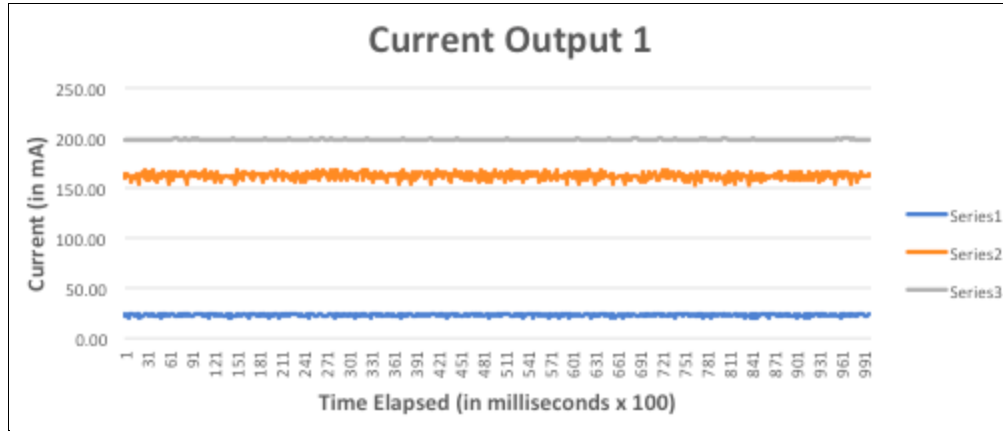


Figure 90. Diagonal Trial 1

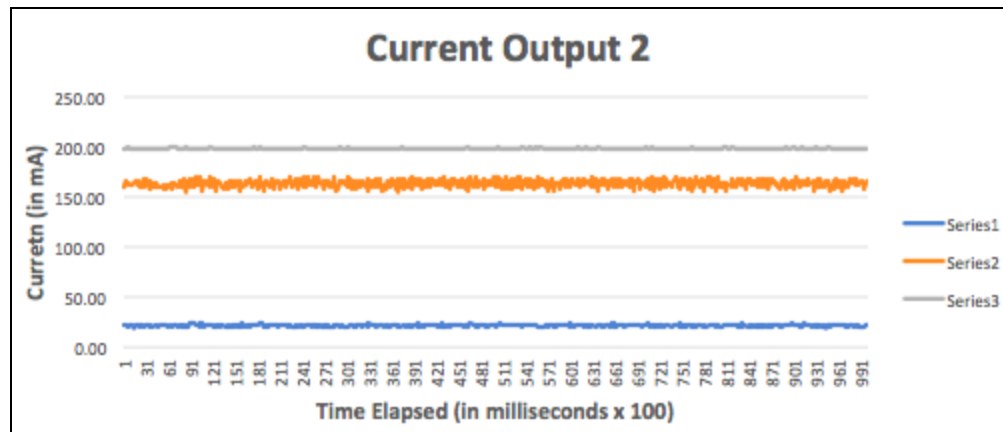


Figure 91. Diagonal Trial 2

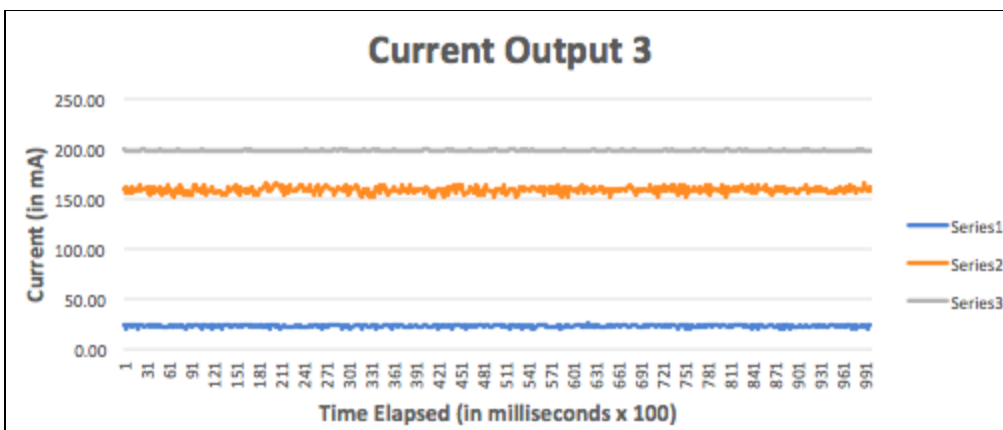


Figure 92. Diagonal Trial 3

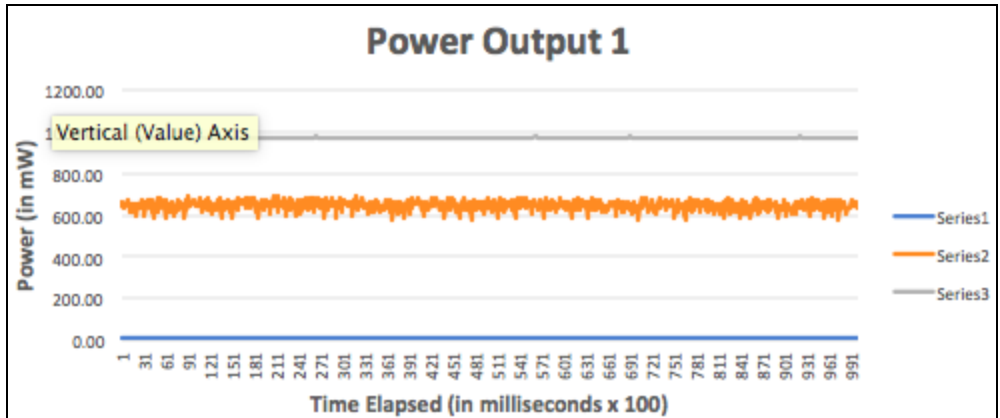


Figure 93. Diagonal Trial 1

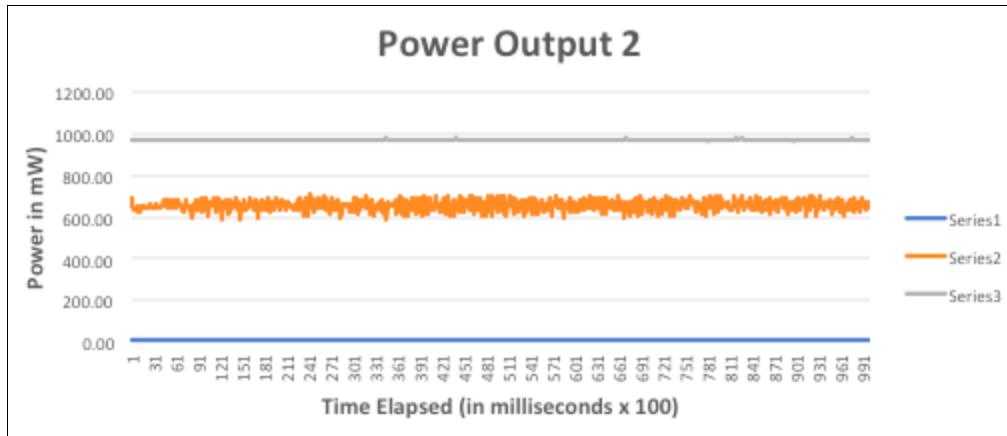


Figure 94. Diagonal Trial 2

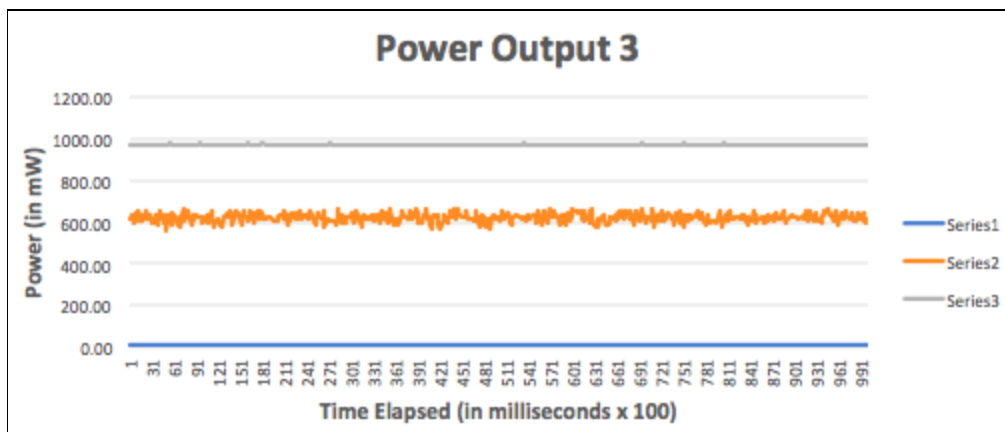


Figure 95. Diagonal Trial 3

References

- [1] Basics of Wind Energy. (n.d.). Retrieved June 11, 2019, from <https://www.awea.org/wind-101/basics-of-wind-energy>.
- [2] U.S Energy Facts Explained. (2018, May 16). Retrieved from https://www.eia.gov/energyexplained/?page=us_energy_home
- [3] (n.d.) Retrieved June 10, 2019, from <https://www.britannica.com/technology/wind-turbine/images-videos/media/1/645101/125134>.
- [4] Where Wind Power Is Harnessed. (n.d.). Retrieved June 11, 2019, from https://www.eia.gov/energyexplained/index.php?page=wind_where.
- [5] Li, S., & Alexander, J. I. (2012, November 09). Optimization of Wind Turbine Array Performance in Offshore Wind Farms. Retrieved June 11, 2019, from <http://proceedings.asmedigitalcollection.asme.org/proceeding.aspx?articleid=1751476>.
- [6] Meneveau, C. (n.d.). Fluid Mechanics and Turbulence in the Wind-Turbine Array Boundary Layer. Retrieved June 11, 2019, from <https://cnls.lanl.gov/~chertkov/SmarterGrids/Talks/Meneveau.pdf>.
- [7] Patel, M. R. (1999). Wind and solar power systems. Boca Raton, FL: CRC Press.
- [8] Ammara I, Leclerc C, Masson C. A viscous three-dimensional differential/actuator-disk method for the aerodynamic analysis of wind farms. *Journal of Solar Energy Engineering* 114 2002; 124:345–56.